horn and gracile nucleus following sciatic nerve injury in the adult rat. *Neuroscience 68*, 167–179.

Martin, D., & Near, S. L. (1995). Protective effect of the interleukin-1 receptor antagonist (IL-1ra) on experimental allergic encephalomyelitis in rats. *J Neuroimmunol 61*, 241–245.

Marz, P., Heese, K., Dimitriades-Schmutz, B., Rose-John, S., & Otten, U. (1999). Role of interleukin-6 and soluble IL-6 receptor in region-specific induction of astrocytic differentiation and neurotrophin expression. *Glia 26*, 191–200.

Meistrell III, M. E., Botchkina, G. I., Wang, H., Di Santo, E., Cockroft, K. M., Bloom, O., et al. (1997). Tumor necrosis factor is a brain damaging cytokine in cerebral ischemia. *Shock 8*, 341–348.

Merrill, J. E., & Benveniste, E. N. (1996). Cytokines in inflammatory brain lesions: helpful and harmful. *Trends Neurosci 19*, 331–338.

Milligan, E. D., Twining, C., Chacur, M., Biedenkapp, J., O'Connor, K., Poole, S., et al. (2003). Spinal glia and proinflammatory cytokines mediate mirror-image neuropathic pain in rats. *J Neurosci 23*, 1026–1040.

Minami, M., Kuraishi, K., Yabuuchi, K., Yamazaki, K., & Satoh, M. (1992). Induction of interleukin-1β mRNA in rat brain transient forebrain ischaemia. *J Neurochem 58*, 390–392.

Moller, T., Kann, O., Verkhratsky, A., & Kettenmann, H. (2000). Activation of mouse microglial cells affects P2 receptor signaling. *Brain Res 853*, 49–59.

Molliver, D. C., Cook, S. P., Carlsten, J. A., Wright, D. E., & Mccleskey, E. W. (2002). ATP and UTP excite sensory neurons and induce CREB phosphorylation through the metabotropic receptor, P2Y2. *Eur J Neurosci 16*, 1850–1860.

Morigiwa, K., Quan, M., Murakami, M., Yamashita, M., & Fukuda, Y. (2000). P2 Purinoceptor expression and functional changes of hypoxia-activated cultured rat retinal microglia. *Neurosci Lett 282*, 153–156.

Moriguchi, S., Mizoguchi, Y., Tomimatsu, Y., Hayashi, Y., Kadowaki, T., Kagamiishi, Y., et al. (2003). Potentiation of NMDA receptor-mediated synaptic responses by microglia. *Brain Res Mol Brain Res 119*, 160–169.

Moriyama, T., Iida, T., Kobayashi, K., Higashi, T., Fukuoka, T., Tsumura, H., et al. (2003). Possible involvement of P2Y2 metabotropic receptors in ATP-induced transient receptor potential vanilloid receptor 1-mediated thermal hypersensitivity. *J Neurosci 23*, 6058–6062.

Myers, R., Manjil, L. G., Cullen, B. M., Price, G. W., Frackowiak, R. S. J., & Cremer, J. E. (1991a). Macrophage and astrocyte populations in relation to [3H] PK11195 binding in rat cerebral cortex following a local ischaemic lesion. *J Cereb Blood Flow Metab 11*, 314–322.

Myers, R., Manjil, L. G., Cullen, B. M., Price, G. W., Frackowiak, R. S. J., & Cremer, J. E. (1991b). (3H) PK 11195 and the localisation of secondary thalamic lesions following focal ischemia in rat motor cortex. *Neurosci Lett 133*, 20–24.

Myers, R., Gunn, R. N., Cunningham, V. J., Banati, R. B., & Jones, T. (1999). Cluster analysis and the reference tissue model in the analysis of clinical [11C](*R*)-PK11195 PET. *J Cereb Blood Flow Metab 19*(Suppl.), 789.

Nagata, K., Nakajima, K., & Kohsaka, S. (1993). Plasminogen promotes the development of rat mesencephalic dopaminergic neurons in vitro. *Brain Res Dev Brain Res 75*, 31–37.

Nakajima, K., & Kohsaka, S. (2001). Microglia: activation and their significance in the central nervous system. *J Biochem (Tokyo) 130*, 169–175.

Nakajima, K., Nagata, K., Hamanoue, M., Takemoto, N., & Kohsaka, S. (1993). Microglia-derived elastase produces a low-molecular-weight plasminogen that enhances neurite outgrowth in rat neocortical explant cultures. *J Neurochem 61*, 2155–2163.

Neary, J. T., Kang, Y., Bu, Y., Yu, E., Akong, K., & Peters, C. M. (1999). Mitogenic signaling by ATP/P2Y purinergic receptors in astrocytes: involvement of a calcium-independent protein kinase C, extracellular signal-regulated protein kinase pathway distinct from the phosphatidylinositol-specific phospholipase C/calcium pathway. *J Neurosci 19*, 4211–4220.

Nörenberg, W., Langosch, J. M., Gebicke-Haerter, P. J., & Illes, P. (1994). Characterization and possible function of adenosine 5′-triphosphate receptors in activated rat microglia. *Br J Pharmacol 111*, 942–950.

Norris, J. G., Tang, L. P., Sparacio, S. M., & Benveniste, E. N. (1994). Signal transduction pathways mediating astrocyte IL-6 induction by IL-1 beta and tumor necrosis factor-alpha. *J Immunol 152*, 841–850.

North, R. A. (2002). Molecular physiology of P2X receptors. *Physiol Rev 82*, 1013–1067.

Ohsawa, K., Imai, Y., Nakajima, K., & Kohsaka, S. (1997). Generation and characterization of a microglial cell line, MG5, derived from a p53-deficient mouse. *Glia 21*, 285–298.

Ohsawa, K., Imai, Y., Kanazawa, H., Sasaki, Y., & Kohsaka, S. (2000). Involvement of Iba1 in membrane ruffling and phagocytosis of macrophages/microglia. *J Cell Sci 113*(Pt 17), 3073–3084.

Ohtori, S., Takahashi, K., Moriya, H., & Myers, R. R. (2004). TNF-alpha and TNF-alpha receptor type 1 upregulation in glia and neurons after peripheral nerve injury: studies in murine DRG and spinal cord. *Spine 29*, 1082–1088.

Onda, A., Murata, Y., Rydevik, B., Larsson, K., Kikuchi, S., & Olmarker, K. (2004). Infliximab attenuates immunoreactivity of brain-derived neurotrophic factor in a rat model of herniated nucleus pulposus. *Spine 29*, 1857–1861.

Pappata, S., Levasseur, M., Gunn, R. N., Myers, R., Crouzel, C., Syrota, A., et al. (2000). Thalamic microglial activation in ischemic stroke detected in vivo by PET and [11C] PK11195. *Neurology 55*, 1052–1054.

Pashenkov, M., Efendic, S., Zhu, J., Zou, L. P., Ostenson, C. G., & Mustafa, M. (2000). Augmented expression of daintain/allograft inflammatory factor-1 is associated with clinical disease: dynamics of daintain/allograft inflammatory factor-1 expression in spleen, peripheral nerves and sera during experimental autoimmune neuritis. *Scand J Immunol 52*, 117–122.

Pasinelli, P., Borchelt, D. R., Houseweart, M. K., Cleveland, D. W., & Brown, R. H., Jr. (1999). Caspase-1 is activated in neuronal cells and tissue with amyotrophic lateral sclerosis-associated mutations in copper–zinc superoxide dismutase. *Proc Natl Acad Sci U S A 95*, 15763–15768.

Perregaux, D., & Gabel, C. A. (1994). Interleukin-1 maturation and release in response to ATP and nigericin. *J Biol Chem 269*, 15195–15203.

Perry, V. H. (1994). Modulation of microglia phenotype. *Neuropathol Appl Neurobiol 20*, 177.

Pollock, J., McFarlane, S. M., Connell, M. C., Zehavi, U., Vandenabeele, P., MacEwan, D. J., et al. (2002). TNF-alpha receptors simultaneously activate Ca2+ mobilisation and stress kinases in cultured sensory neurones. *Neuropharmacology 42*, 93–106.

Raghavendra, V., Tanga, F., & Deleo, J. A. (2003). Inhibition of microglial activation attenuates the development but not existing hypersensitivity in a rat model of neuropathy. *J Pharmacol Exp Ther 306*, 624–630.

Ramsay, S. C., Weiller, C., Myers, R., Cremer, J. E., Luthra, S. K., Lammertsma, A. A., et al. (1992). Monitoring by PET of macrophage accumulation in brain after ischaemic stroke. *Lancet 339*, 1054–1055.

Relton, J. K., & Rothwell, N. J. (1992). Interleukin-1 receptor antagonist inhibits ischaemic and excitotoxic neuronal damage in the rat. *Brain Res Bull 29*, 243–246.

Robertson, B., Xu, X. J., Hao, J. X., Wiesenfeld-Hallin, Z., Mhlanga, J., Grant, G., et al. (1997). Interferon-gamma receptors in nociceptive pathways: role in neuropathic pain-related behaviour. *NeuroReport 8*, 1311–1316.

Robinson, A. P., White, T. M., & Mason, D. W. (1986). Macrophage heterogeneity in the rat as delineated by two monoclonal antibodies MRC OX-41 and MRC OX-42, the latter recognizing complement receptor type 3. *Immunology 57*, 239–247.

Rothwell, N. J. (1999). Cytokines: killers in the brain? *J Physiol (Lond) 514*, 3–17.

Rothwell, N., Allan, S., & Toulmond, S. (1997). The role of interleukin 1 in acute neurodegeneration and stroke: pathophysiological and therapeutic implications. *J Clin Invest 100*, 2648–2652.

Sanada, M., Yasuda, H., Omatsu-Kanbe, M., Sango, K., Isono, T., Matsuura, H., et al. (2002). Increase in intracellular Ca(2+) and calcitonin gene-related peptide release through metabotropic P2Y receptors in rat dorsal root ganglion neurons. *Neuroscience 111*, 413–422.

Sanz, J. M., & Di Virgilio, F. (2000). Kinetics and mechanism of ATP-dependent IL-1 beta release from microglial cells. *J Immunol 164*, 4893–4898.

Sawada, M., Hara, N., & Maeno, T. (1990). Extracellular tumor necrosis factor induces a decreased K+ conductance in an identified neuron of *Aplysia kurodai*. *Neurosci Lett 115*, 219–225.

Sawada, M., Suzumura, A., & Marunouchi, T. (1992). TNF alpha induces IL-6 production by astrocytes but not by microglia. *Brain Res 583*, 296–299.

Schäfers, M., Geis, C., Brors, D., Yaksh, T. L., & Sommer, C. (2002). Anterograde transport of tumor necrosis factor-alpha in the intact and injured rat sciatic nerve. *J Neurosci 22*, 536–545.

Schäfers, M., Lee, D. H., Brors, D., Yaksh, T. L., & Sorkin, L. S. (2003). Increased sensitivity of injured and adjacent uninjured rat primary sensory neurons to exogenous tumor necrosis factor-alpha after spinal nerve ligation. *J Neurosci 23*, 3028–3038.

Schäfers, M., Svensson, C. I., Sommer, C., & Sorkin, L. S. (2003). Tumor necrosis factor-alpha induces mechanical allodynia after spinal nerve ligation by activation of p38 MAPK in primary sensory neurons. *J Neurosci 23*, 2517–2521.

Scherbel, U., Raghupathi, R., Nakamura, M., Saatman, K. E., Trojanowski, J. Q., Neugebauer, E., et al. (1999). Differential acute and chronic responses of tumor necrosis factor-deficient mice to experimental brain injury. *Proc Natl Acad Sci U S A 96*, 8721–8726.

Schijver, H. M., Crusius, J. B., Uitdehaag, B. M., Gonzalez, M. A., Kostense, P. J., Polman, C. H., et al. (1999). Association of interleukin-1beta and interleukin-1 receptor antagonist genes with disease severity in MS. *Neurology 52*, 595–599.

Sette, G., Baron, J. C., Young, A. R., Miyazawa, H., Tillet, I., Barre, L., et al. (1993). In vivo mapping of brain benzodiazepine receptor changes by positron emission tomography after focal ischemia in the anesthetized baboon. *Stroke 24*, 2046–2057.

Shigemoto-Mogami, Y., Koizumi, S., Tsuda, M., Ohsawa, K., Kohsaka, S., & Inoue, K. (2001). Mechanisms underlying extracellular ATP-evoked interleukin-6 release in mouse microglial cell line, MG-5. *J Neurochem 78*, 1339–1349.

Soliven, B., & Albert, J. (1992). Tumor necrosis factor modulates Ca2+ currents in cultured sympathetic neurons. *J Neurosci 12*, 2665–2671.

Solle, M., Labasi, J., Perregaux, D. G., Stam, E., Petrushova, N., & Koller, B. H. (2001). Altered cytokine production in mice lacking P2X(7) receptors. *J Biol Chem 276*, 125–132.

Sommer, C., & Schäfers, M. (1998). Painful mononeuropathy in C57BL/Wld mice with delayed Wallerian degeneration: differential effects of cytokine production and nerve regeneration on thermal and mechanical hypersensitivity. *Brain Res 784*, 154–162.

Sommer, C., Marziniak, M., & Myers, R. R. (1998). The effect of thalidomide treatment on vascular pathology and hyperalgesia caused by chronic constriction injury of rat nerve. *Pain 74*, 83–91.

Sommer, C., Schäfers, M., Marziniak, M., & Toyka, K. V. (2001). Etanercept reduces hyperalgesia in experimental painful neuropathy. *J Peripher Nerv Syst 6*, 67–72.

Sommer, C., Lindenlaub, T., Teuteberg, P., Schäfers, M., Hartung, T., & Toyka, K. V. (2001). Anti-TNF-neutralizing antibodies reduce pain-related behavior in two different mouse models of painful mononeuropathy. *Brain Res 913*, 86–89.

Sorkin, L. S., & Doom, C. M. (2000). Epineurial application of TNF elicits an acute mechanical hyperalgesia in the awake rat. *J Peripher Nerv Syst 5*, 96–100.

Sorkin, L. S., Xiao, W. H., Wagner, R., & Myers, R. R. (1997). Tumour necrosis factor-alpha induces ectopic activity in nociceptive primary afferent fibres. *Neuroscience 81*, 255–262.

Stoll, G., & Jander, S. (1999). The role of microglia and macrophages in the pathophysiology of the CNS. *Prog Neurobiol 58*, 233–247.

Streit, W. J., Walter, S. A., & Pennell, N. A. (1999). Reactive microgliosis. *Prog Neurobiol 57*, 563–581.

Stuesse, S. L., Cruce, W. L., Lovell, J. A., Mcburney, D. L., & Crisp, T. (2000). Microglial proliferation in the spinal cord of aged rats with a sciatic nerve injury. *Neurosci Lett 287*, 121–124.

Surprenant, A., Rassendren, F., Kawashima, E., North, R. A., & Buell, G. (1996). The cytolytic P2Z receptor for extracellular ATP identified as a P2X receptor (P2X7). *Science 272*, 735–738.

Suzuki, T., Hide, I., Ido, K., Kohsaka, S., Inoue, K., & Nakata, Y. (2004). Production and release of neuroprotective tumor necrosis factor by P2X7 receptor-activated microglia. *J Neurosci 24*, 1–7.

Svichar, N., Shmigol, A., Verkhratsky, A., & Kostyuk, P. (1997). ATP induces Ca2+ release from IP3-sensitive Ca^{2+} stores exclusively in large DRG neurones. *NeuroReport 8*, 1555–1559.

Sweitzer, S., Martin, D., & Deleo, J. A. (2001). Intrathecal interleukin-1 receptor antagonist in combination with soluble tumor necrosis factor receptor exhibits an anti-allodynic action in a rat model of neuropathic pain. *Neuroscience 103*, 529–539.

Tanaka, S., & Koike, T. (2002). Selective inflammatory stimulations enhance release of microglial response factor (MRF)-1 from cultured microglia. *Glia 40*, 360–371.

Tanaka, S., Suzuki, K., Watanabe, M., Matsuda, A., Tone, S., & Koike, T. (1998). Upregulation of a new microglial gene, mrf-1, in response to programmed neuronal cell death and degeneration. *J Neurosci 18*, 6358–6369.

Tanaka, S., Kato, H., & Koike, T. (2000). Microglial response factor (MRF)-1: constitutive expression in ramified microglia and upregulation upon neuronal death induced by ischemia or glutamate exposure. *Zool Sci 17*, 571–578.

Thompson, S. W., Bennett, D. L., Kerr, B. J., Bradbury, E. J., & Mcmahon, S. B. (1999). Brain-derived neurotrophic factor is an endogenous modulator of nociceptive responses in the spinal cord. *Proc Natl Acad Sci U S A 96*, 7714–7718.

Toescu, E. C., Moller, T., Kettenmann, H., & Verkhratsky, A. (1998). Long-term activation of capacitative Ca2+ entry in mouse microglial cells. *Neuroscience 86*, 925–935.

Tominaga, M., Wada, M., & Masu, M. (2001). Potentiation of capsaicin receptor activity by metabotropic ATP receptors as a possible mechanism for ATP-evoked pain and hyperalgesia. *Proc Natl Acad Sci U S A 98*, 6951–6956.

Tsuda, M., Koizumi, S., Kita, A., Shigemoto, Y., Ueno, S., & Inoue, K. (2000). Mechanical allodynia caused by intraplantar injection of P2X receptor agonist in rats: involvement of heteromeric P2X2/3 receptor signaling in capsaicin-insensitive primary afferent neurons. *J Neurosci 20*, RC90.

Tsuda, M., Shigemoto-Mogami, Y., Koizumi, S., Mizokoshi, A., Kohsaka, S., Salter, M. W., et al. (2003). P2X4 receptors induced in spinal microglia gate tactile allodynia after nerve injury. *Nature 424*, 778–783.

Tsuda, M., Mizokoshi, A., Shigemoto-Mogami, Y., Koizumi, S., & Inoue, K. (2004). Activation of p38 mitogen-activated protein kinase in spinal hyperactive microglia contributes to pain hypersensitivity following peripheral nerve injury. *Glia 45*, 89–95.

Tsuda, M., Inoue, K., & Salter, M. W. (2005). Neuropathic pain and spinal microglia: a big problem from molecules in 'small' glia. *Trends Neurosci 28*, 101–107.

Ueno, S., Tsuda, M., Iwanaga, T., & Inoue, K. (1999). Cell type-specific ATP-activated responses in rat dorsal root ganglion neurons. *Br J Pharmacol 126*, 429–436.

Utans, U., Arceci, R. J., Yamashita, Y., & Russell, M. E. (1995). Cloning and characterization of allograft inflammatory factor-1: a novel macrophage factor identified in rat cardiac allografts with chronic rejection. *J Clin Invest 95*, 2954–2962.

Vezzani, A., Conti, M., De Luigi, A., Ravizza, T., Moneta, D., Marchesi, F., et al. (1999). Interleukin-1 beta immunoreactivity and microglia are enhanced in the rat hippocampus by focal kainate application: functional evidence for enhancement of electrographic seizures. *J Neurosci 19*, 5054–5065.

Vezzani, A., Moneta, D., Conti, M., Richichi, C., Ravizza, T., De Luigi, A., et al. (2000). Powerful anticonvulsant action of IL-1 receptor antagonist on intracerebral injection and astrocytic overexpression in mice. *Proc Natl Acad Sci U S A 97*, 11534–11539.

Vikman, K. S., Hill, R. H., Backstrom, E., Robertson, B., & Kristensson, K. (2003). Interferon-gamma induces characteristics of central sensitization in spinal dorsal horn neurons in vitro. *Pain 106*, 241–251.

Visentin, S., Renzi, M., Frank, C., Greco, A., & Levi, G. (1999). Two different ionotropic receptors are activated by ATP in rat microglia. *J Physiol 519*, 723–736.

Viviani, B., Bartesaghi, S., Gardoni, F., Vezzani, A., Behrens, M. M., Bartfai, T., et al. (2003). Interleukin-1beta enhances NMDA receptor-mediated intracellular calcium increase through activation of the Src family of kinases. *J Neurosci 23*, 8692–8700.

Wagner, R., & Myers, R. R. (1996). Endoneurial injection of TNF-alpha produces neuropathic pain behaviors. *NeuroReport 7*, 2897–2901.

Walz, W., Ilschner, S., Ohlemeyer, C., Banati, R., & Kettenmann, H. (1993). Extracellular ATP activates a cation conductance and a K+ conductance in cultured microglial cells from mouse brain. *J Neurosci 13*, 4403–4411.

Wang, S., Cheng, Q., Malik, S., & Yang, J. (2000). Interleukin-1beta inhibits gamma-aminobutyric acid type A (GABA(A)) receptor current in cultured hippocampal neurons. *J Pharmacol Exp Ther 292*, 497–504.

Watkins, L. R., Milligan, E. D., & Maier, S. F. (2001). Glial activation: a driving force for pathological pain. *Trends Neurosci 24*, 450–455.

Winkelstein, B. A., Rutkowski, M. D., Sweitzer, S. M., Pahl, J. L., & Deleo, J. A. (2001). Nerve injury proximal or distal to the DRG induces similar spinal glial activation and selective cytokine expression but differential behavioral responses to pharmacologic treatment. *J Comp Neurol 439*, 127–139.

Woods, T. M., Cusick, C. G., Pons, T. P., Taub, E., & Jones, E. G. (2000). Progressive transneuronal changes in the brainstem and thalamus after long-term dorsal rhizotomies in adult macaque monkeys. *J Neurosci 20*, 3384–3399.

Woolf, C. J., & Salter, M. W. (2000). Neuronal plasticity: increasing the gain in pain. *Science 288*, 1765–1769.

Yamasaki, Y., Suzuki, T., Yamaya, H., Matsuura, N., Onodera, H., & Kogure, K. (1992). Possible involvement of interleukin-1 in ischemic brain edema formation. *Neurosci Lett 142*, 45–47.

Yang, L., Lindholm, K., Konishi, Y., Li, R., & Shen, Y. (2002). Target depletion of distinct tumor necrosis factor receptor subtypes reveals hippocampal neuron death and survival through different signal transduction pathways. *J Neurosci 22*, 3025–3032.

Yu, X. M., Askalan, R., Keil II, G. J., & Salter, M. W. (1997). NMDA channel regulation by channel-associated protein tyrosine kinase Src. *Science 275*, 674–678.

Available online at www.sciencedirect.com
SCIENCE DIRECT®
ELSEVIER
Diabetes Research and Clinical Practice 68 (2005) 117–125
DIABETES RESEARCH AND CLINICAL PRACTICE
www.elsevier.com/locate/diabres

Osteoclastic function is accelerated in male patients with type 2 diabetes mellitus: the preventive role of osteoclastogenesis inhibitory factor/osteoprotegerin (OCIF/OPG) on the decrease of bone mineral density

Kiyoshi Suzuki[a,c], Takeshi Kurose[c], Makoto Takizawa[a], Masahiro Maruyama[a], Kenji Ushikawa[a], Munetsugu Kikuyama[c], Chieko Sugimoto[c], Yutaka Seino[d], Shinya Nagamatsu[b], Hitoshi Ishida[a,*]

[a]*Third Department of Internal Medicine, Kyorin University School of Medicine, 6-20-2 Shinkawa, Mitaka, Tokyo 181-8611, Japan*
[b]*Second Department of Biochemistry, Kyorin University School of Medicine, Mitaka, Tokyo 181-8611, Japan*
[c]*Department of Internal Medicine, Shimada Municipal Hospital, Shimada, Shizuoka 427-8502, Japan*
[d]*Department of Metabolism and Clinical Nutrition, Kyoto University School of Medicine, Sakyo-ku, Kyoto 606-8507, Japan*

Received 9 December 2003; received in revised form 28 July 2004; accepted 19 August 2004
Available online 12 October 2004

Abstract

To clarify the pathogenesis of altered bone metabolism in diabetic state and its underlying mechanisms, the bone mineral content and fasting levels of serum intact parathyroid hormone (i-PTH), intact osteocalcin (i-OC), tartrate-resistant acid phosphatase (TRAP) and osteoclastgenesis inhibitory factor/osteoprotegerin (OCIF/OPG) were measured in male type 2 diabetic patients and their age-matched controls. In addition, urine levels of osteoclastic markers, C-telopeptide of type I collagen (CTx), deoxypyridinoline (DPD), and N-telopeptide of type I collagen (NTx) were simultaneously determined. Serum levels of i-PTH and i-OC in diabetic patients were significantly lower than those in the controls. Conversely, serum concentrations of TRAP were significantly elevated in diabetic patients. However, no clear correlation was observed between serum i-OC and TRAP. It was also observed that urinary excretion of CTx, DPD, and NTx was significantly increased in the diabetics as compared with the controls. Unexpectedly, serum levels of OCIF/OPG tended to be higher in the diabetic group, and these values exhibited a significantly positive correlation with those of serum TRAP. There was found a significantly negative correlation between serum TRAP and bone mineral density (BMD) and also between serum OCIF/OPG and bone mineral

* Corresponding author. Tel.: +81 422 47 5511x5822; fax: +81 422 76 6451.
E-mail address: ishida@kyorin-u.ac.jp (H. Ishida).

0168-8227/$ – see front matter
doi:10.1016/j.diabres.2004.08.006

density. It seems probable that OCIF/OPG has a suppressive role on the increased bone resorption to prevent further loss of the skeletal bone mass in type 2 diabetic patients.

Keywords: Type 2 diabetes mellitus; Intact osteocalcin; Bone resorption; Tartrate-resistant acid phosphatase (TRAP); Osteoclastogenesis inhibitory factor/osteoprotegerin (OCIF/OPG)

1. Introduction

It has been recognized that the alterations in mineral and bone metabolism are associated with diabetes mellitus and that the resulting bone loss is one of the chronic complications of diabetic patients [1–6]. Regarding the altered bone metabolism found in patients with type 2 diabetes, we and others have demonstrated the evidence that the osteoblastic function was decreased whereas the osteoclastic function was conversely elevated [5,7,8]. In order to further confirm the enhancement of osteoclastic function in type 2 diabetes, we measured the urine markers for bone resorption, cross-linked C-telopeptide of type I collagen (CTx), deoxypyridinoline (DPD), and cross-linked N-telopeptide of type I collagen (NTx) [9–11], as well as the circulating osteoclastic marker.

In terms of the molecular mechanisms for functional coupling between osteoblasts and osteoclasts, the bone coupling factors have been recently cloned from osteoblastic cells. Osteoclast differentiation factor (ODF) has been identified as a membrane-bound ligand mediating an essential signal to osteoclast progenitors for their differentiation into osteoclasts [12,13]. On the other hand, osteoclastogenesis inhibitory factor/osteoprotegerin (OCIF/OPG) inhibits the osteoclastogenesis by interrupting the binding of ODF to ODF receptor of osteoclast progenitors [14,15].

In this study, we confirmed that the osteoclastic function is significantly accelerated in type 2 diabetic patients. For the purpose of clarifying its underlying pathogenesis, the circulating levels of OCIF/OPG were measured to investigate their interrelationship with the increased osteoclastic markers, and then the putative role of OCIF/OPG on the altered bone metabolism in diabetes was analyzed.

2. Subjects

A total of 169 male type 2 diabetic patients (55. ± 0.9 years of age and 6.1 ± 0.5 years of disease duration; means ± S.E.) was examined in this study. Ninety-five age-matched male healthy subjects (54.7 ± 1.1 years of age) were also studied as the controls with fasting blood glucose level less than 7.0 mmol/l (Table 1). The female type 2 diabetic patients were excluded from the present study to prevent the influences of sex hormones from the evaluations of bone mineral content. Those who had obvious renal dysfunction (serum creatinine levels of 1.32 ± 10^{-4} mmol/l or more, urine corrected albumin levels

Table 1
Clinical profile of male patients with type 2 diabetes and their age-matched controls

	Number	Body mass index (kg/m^2)	Duration (years)	Glucose (nmol/l)	HbA1c (%)
Diabetic patients					
Diet	61	23.5 ± 0.5	5.4 ± 0.9	9.37 ± 0.51[a]	8.3 ± 0.3[a]
Oral hypoglycemic agent	64	21.8 ± 0.4[b]	6.5 ± 0.8	10.41 ± 0.48[a]	10.1 ± 0.3[a]
Insulin	44	21.0 ± 0.5[a]	7.0 ± 0.9	12.43 ± 0.66[a]	10.6 ± 0.4[a]
Totals	169	22.3 ± 0.2	6.1 ± 0.5	10.46 ± 0.29[a]	10.0 ± 0.5[a]
Controls	95	22.8 ± 0.2	–	5.41 ± 0.05	5.0 ± 0.1

Values were presented as mean ± S.E.
[a] $p < 0.01$.
[b] $p < 0.05$ vs. controls.

of 5.04 ± 10^{-6} mg/mmol creatinine or more) were excluded to avoid possible influence of renal osteodystrophy and retardation of hormone excretion [16]. In addition, the patients with retinopathy, neuropathy and coronary artery disease were also excluded. None had taken oral calcium supplementation, drugs such as statins to affect bone metabolism [17] or any vitamin preparation containing Vitamin D, or K. Each subjects had given informed written consent to participate in this study, and the study was carried out in accordance with the Declaration of Helsinki as revised in 1996.

3. Methods

3.1. Biochemistry

A Hitachi 7350 autoanalyzer (Hitachi Co. Ltd., Tokyo, Japan) was used to measure circulating levels of glucose, calcium, magnesium, inorganic phosphorus, creatinine and albumin, and urinary excretion of calcium and creatinine. Corrected values of serum calcium were calculated according to the formula $10y/x$ mmol/g albumin, where x denotes albumin (g/dl) and y denotes calcium (mmol/l) [18]. HbA1c was determined with a high-performance liquid chromatography [19]. Urine C-peptide (CPR) was analyzed by a radioimmunoassay (RIA) technique as reported previously [20]. Serum insulin was determined by enzyme immunoassay (AxSYM Insulin Kit, Dinabott Co. Ltd., Tokyo, Japan) using monoclonal antibody which cross-reacted neither with human proinsulin nor CPR. The sensitivity of this assay is 1.0 pmol/l, and the coefficients of variance (CV) of intra- and inter-assay were 2.2–2.7% and 3.5–7.2%, respectively. Serum intact osteocalcin (i-OC) was determined by one-step enzyme immunometric assay (Osteocalcin test Teijin, Teijin Co. Ltd. Tokyo, Japan) [21]. The sensitivity of this assay is 8.5 pmol/l, and the CV of intra- and inter-assay were 2.5–7.5% and 4.0–7.6%, respectively. Serum TRAP was determined by using paranitrophenol phosphate as previously described [22]. Intact molecules of parathyroid hormone (i-PTH) in serum were determined by a highly sensitive two-site immunoradiometric assay [6]. The detection limit for i-PTH was 10 pmol/l, and CV of intra- and inter-assay were 2.6–2.9% and 3.0–4.0%, respectively. Circulating 1,25 dihydroxyvitamin D_3 ($1,25(OH)_2D_3$) were measured by RIA ($1,25(OH)_2D$ RIA Kit; Immunodiagnostic Systems Co. Ltd., Boldon, UK) [23]. The sensitivity of this assay is 3.3 pmol/ml, and the CV of intra- and inter-assay were 8.7–10.4% and 11.3–11.9%, respectively.

Urinary concentrations of CTx were quantified by RIA (α-CrossLaps®; Osteometer Co. Ltd., Copenhagen, Denmark) using a specific monoclonal antibody [9]. The detection limit for CTx is 44 nmol/l, and CV of the intra- and inter-assay were 2.9–9.7% and 4.6–9.6%, respectively. Urinary DPD were quantified by ELISA (Osteolinks "D"®; Sumitomo Pharmaceutical Co. Ltd., Osaka, Japan) using a specific monoclonal antibody [10]. The detection limit for DPD is 1.1 nmol and CV of the intra- and inter-assay were 3.5–4.3% and 4.4–5.7%, respectively. The DPD assay used determines only the free component of DPD in urine since samples are not hydrolysed. Urinary NTx were measured using ELISA assay (Osteomark®, Ostex International Inc., Seattle, WA) and were expressed as nanomoles of bone collagen equivalent (BCE)/l/mM creatinine [11]. The detection limit for NTx is 5.0 nMBCE/mMcre, and CV of the intra- and inter-assay were 3.5–4.4% and 2.9–4.8%, respectively.

Serum levels of OCIF/OPG were determined by two steps sandwich ELISA (OCIF/OPG Kit; Cosmo Bio. Co. Ltd., Tokyo, Japan) according to the method of Tsuda et al. [14]. The detection limit for OCIF/OPG is 0.52 pmol/l, and CV of the intra- and inter-assay were 4.3–4.9% and 8.7–10.5%, respectively.

After overnight fasting, blood samples were collected from the antecubital vein and centrifuged at 3000 rpm for 5 min. Serum was immediately separated and stored at −40 °C until assayed. The first morning urine samples were collected and centrifuged at 1500 rpm for 5 min immediately after collection in order to eliminate the debris, and were also stored at −40 °C.

3.2. Measurement of bone mineral density

Teijin Bonalyzer (Teijin Co. Ltd.) was utilized to measure the bone mineral density (BMD) by means of computed X-ray densitometry (CXD) at the center of the right second metacarpal bone [6]. The principle of this method is based on the microdensitometric method using X-ray films of hands with aluminum

step scale as standard [3,4,6]. The index corresponding to bone mineral density (m-BMD) was obtained as the integrated value of the density area in X-ray film derived by the width of metacarpal bone. It was calculated that CV of m-BMD was 1.2–2.0% and m-BMD reflects the cortical density of the metacarpal bone [6].

3.3. Statistical analysis

The results were expressed as the mean ± S.E. Student's unpaired *t*-test and a one-way ANOVA analysis of variance test were used for statistical analysis. To test the relationship between two indices, Spearman's correlation coefficient test was performed. Differences were accepted as significant at $p < 0.05$.

4. Results

4.1. Urinary excretion of CPR, circulating levels of insulin, calcium, inorganic phosphorus, magnesium, i-PTH, 1,25(OH)$_2$D$_3$, and bone mineral density

Table 2 shows urinary excretion of CPR, circulating values of insulin, minerals, i-PTH and 1,25(OH)$_2$D$_3$ along with m-BMD in type 2 diabetic patients and in the controls. Urine levels of CPR were significantly reduced in type 2 diabetic patients compared to those in control subjects ($p < 0.01$). On the other hand, fasting levels of serum insulin tended to be higher in the diabetics, but no statistical difference was observed between the diabetic and control groups. Serum levels of corrected calcium and magnesium were significantly lower in the diabetic group than in the controls ($p < 0.05$–0.01), but serum inorganic phosphorus was not significantly different. Serum i-PTH and 1,25(OH)$_2$D$_3$ were significantly decreased in diabetic patients than in their controls ($p < 0.01$). The values of m-BMD were significantly lower in the diabetic group compared to the control group ($p < 0.05$), indicating the decreased bone mass in the diabetic state.

4.2. Serum i-OC, TRAP, OCIF/OPG and urinary excretion of CTx, DPD, and NTx

Serum level of i-OC in type 2 diabetic patients was 0.53 ± 0.03 nmol/l, which was significantly lower than those in the controls (1.02 ± 0.05 nmol/l, $p < 0.01$). On the other hand, serum levels of TRAP in type 2 diabetic patients were 10.75 ± 0.14 U/l, and were significantly higher than those in the control group (9.50 ± 0.10 U/l, $p < 0.01$) (Fig. 1). Serum OCIF/OPG in diabetic patients (9.05 ± 0.45 pmol/l) tended to be higher than that in the control group (8.00 ± 0.31 pmol/l), although it is not statistically significant ($0.05 < p < 0.1$). In addition, urinary concentrations of CTx, DPD, and NTx in type 2 diabetic patients were 161 ± 8 nmol/mMcre, 4.80 ± 0.13 nmol/mMcre and 41.9 ± 2.0 nMBCE/mMcre, respectively, and were also significantly higher than those in the control group (136 ± 6, 4.13 ± 0.13 nmol/mMcre, and 34.6 ± 1.5 nMBCE/mMcre, respectively; $p < 0.05$–0.01) (Fig. 2).

Table 2
Urine levels of CPR, circulating values of insulin and bone metabolic markers, and bone mineral density in male type 2 diabetic patients and their age-matched controls

	Type 2 diabetics	Controls
Urine CPR (nmol/day)	20.7 ± 1.3[a]	30.0 ± 3.3
Insulin (pmol/l)	46.8 ± 2.5	37.8 ± 3.6
Corrected calcium (mmol/kg albumin)	5.08 ± 0.05[a]	5.31 ± 0.04
Inorganic phosphorus (mmol/l)	1.05 ± 0.01	1.04 ± 0.02
Magnesium (mmol/l)	0.81 ± 0.01[b]	0.83 ± 0.01
Intact PTH (pmol/l)	2.38 ± 0.10[a]	3.26 ± 0.10
1,25 (OH)$_2$D$_3$ (pmol/l)	101.3 ± 5.5[a]	131.9 ± 7.3
m-BMD (mmAl)	2.80 ± 0.15[b]	3.11 ± 0.03

Values were presented as mean ± S.E.
[a] $p < 0.01$.
[b] $p < 0.05$ vs. control.

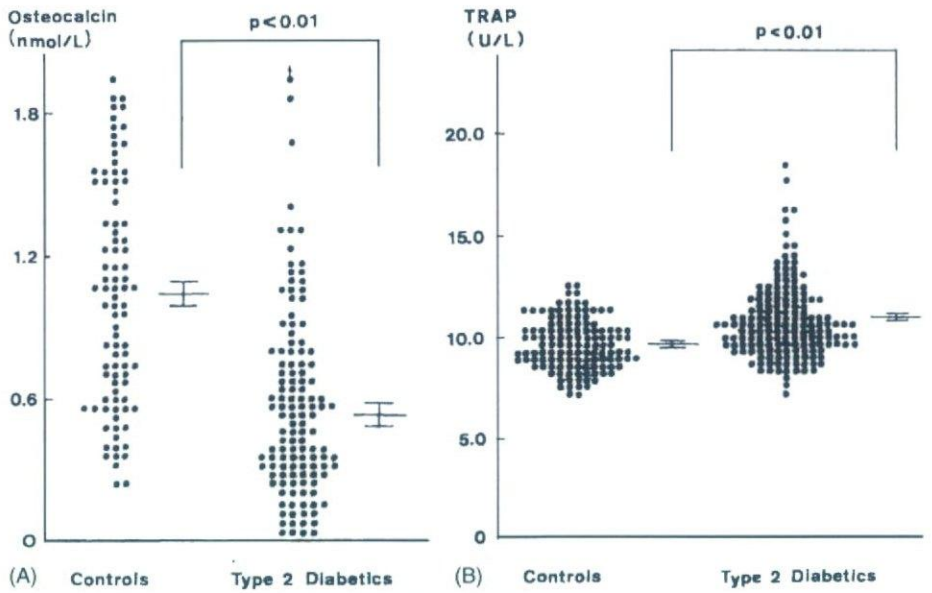

Fig. 1. Serum levels of i-OC (A), and TRAP (B) in type 2 diabetic patients and control subjects. Level of i-OC in the type 2 diabetics was significantly lower than that of the controls ($p < 0.01$). On the other hand, serum level of TRAP in the diabetics was higher than the value in their controls ($p < 0.01$).

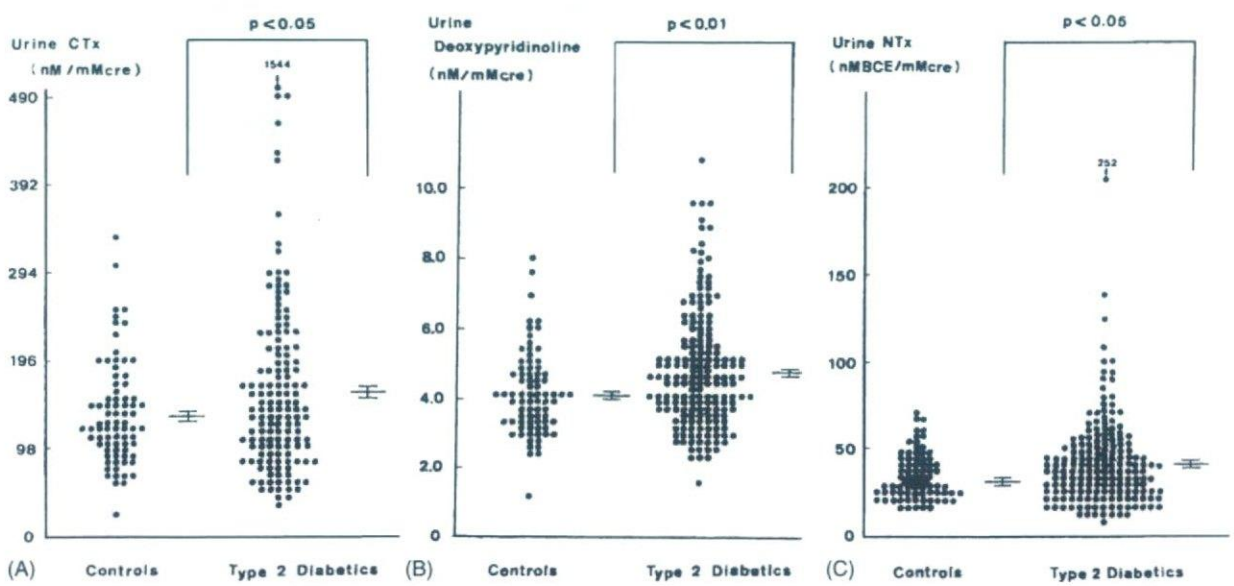

Fig. 2. Urine levels of CTx to creatinine (A), deoxypyridinoline (DPD) to creatinine (B), and NTx to creatinine (C) in type 2 diabetic patients and control subjects. Urine concentration of CTx and NTx in the type 2 diabetics was significantly higher than that in their controls ($p < 0.05$). Urine DPD in the diabetic group was also significantly higher than the value in their control group ($p < 0.01$).

4.3. Correlation coefficients among serum i-PTH and i-OC, serum and urine osteoclastic markers, and m-BMD in diabetic patients

A significantly positive correlation was found in diabetic patients between serum i-PTH and i-OC ($r = 0.289$, $p < 0.01$). There was no clear correlation between serum i-OC and TRAP. On the other hand, serum TRAP exhibited significantly positive correlation with urine osteoclastic markers (CTx and DPD) ($r = 0.298$ and 0.250, respectively; $p < 0.01$). A significantly negative correlation was observed between m-BMD and serum levels of TRAP ($r = -0.254$, $p < 0.01$). The urinary excretion of CTx, DPD, and NTx similarly exhibited a tendency to be negatively correlated with m-BMD ($r = -0.211$, -0.179, and -0.162, respectively).

4.4. Correlationship between serum OCIF/OPG and serum i-OC, TRAP or m-BMD in diabetic patients

There was a significantly positive correlation in diabetic patients between circulating levels of OCIF/OPG and TRAP ($p < 0.01$; Fig. 3). The urinary excretion of CTx and DPD similarly tended to be negatively correlated with serum levels of OCIF/OPG ($r = -0.164$ and -0.103, respectively, $0.05 < p < 0.1$). On the other hand, a significantly negative correlation was found between m-BMD and serum OCIF/OPG ($p < 0.01$). There was no clear correlation between circulating levels of OCIF/OPG and i-OC (Fig. 3).

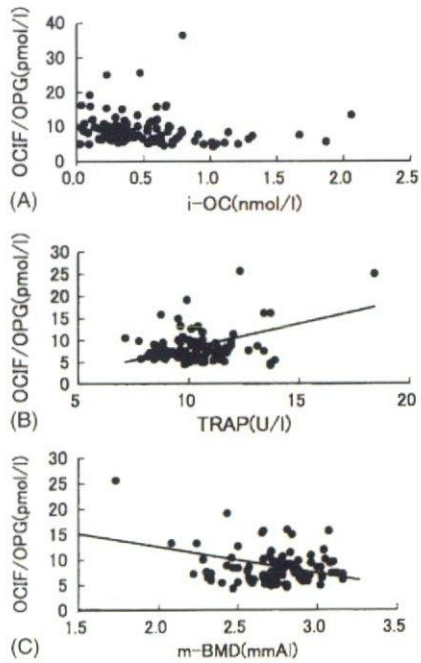

Fig. 3. Correlationship between serum OCIF/OPG (y-axis) and serum i-OC (A), TRAP (B) or m-BMD (C) (x-axis) in diabetic patients. There was a significantly positive correlation between circulating OCIF/OPG and TRAP ($r = 0.344$, $y = 2.72 + 1.10x$, $p < 0.01$), whereas no significant relationship was observed between serum OCIF/OPG and i-OC. On the other hand, a significantly negative correlation was found between serum OCIF/OPG and m-BMD ($r = -0.302$, $y = 22.97 - 5.21x$, $p < 0.01$).

5. Discussion

The existence of diabetic osteopenia and altered mineral metabolism has been recognized as one of the chronic complications of diabetes mellitus [1–8]. In type 1 diabetic patients, fairly uniform results were obtained, where bone mass is reduced by 6–14% in the forearm [4]. Although many reports have been published to elucidate pathophysiological characteristics of abnormal bone metabolism in type 2 diabetic patients, however no detailed consensus on the pathogenesis of osteopenia in type 2 diabetes has been yet obtained. Differences in the race, age, sex and degree of obesity of the subjects in these studies can be considered as the causal factors of this inconsistency [4,24,25]. Therefore, in the present study, only non-obese male patients with type 2 diabetes and their age-matched control subjects were examined in order to prevent the influence of sex, age and obesity from the evaluations of altered bone metabolism. The decreased activity of osteoblasts under diabetic conditions has been commonly observed in both diabetic animals and humans [7,26–28]. Since a positive correlation was found between i-PTH and i-OC, it is speculated that the relative hypofunction of parathyroid gland causes the decreased activity of diabetic osteoblasts. However, it has been still controversial if the osteoclastic function in diabetes is elevated or not [5,7,29,30]. We have previously reported that serum level of osteoblastic osteocalcin was decreased, while circulating TRAP, a bone resorption marker, was conversely elevated in genetically diabetic Wistar fatty rats [20], suggesting

the increased activity of osteoclasts in diabetic state. Moreover, in male type 2 diabetic patients, we found in the present study that serum concentrations of TRAP was significantly higher than those in age-matched controls, and that a significantly negative correlation was observed between serum TRAP and bone mineral content. A significant decrease in serum osteocalcin was conversely observed in the identical cases of type 2 diabetic patients, and there was no clear correlation between i-OC and TRAP. Thus, the accelerated osteoclastic activities and the putative uncoupling between the functions of osteoblasts and of osteoclasts would be supposedly related to the pathogenesis of diabetic osteopenia.

In order to ascertain the fact that osteoclastic activity in diabetic patients is increased, urinary excretion of CTx, DPD, and NTx was simultaneously examined. CTx and NTx have been known to be the cross-linked C- and N-terminal telopeptide of bone type I collagen and to be released into blood stream after the degradation of collagen through osteoclast-derived proteases [31]. Since CTx, DPD, and NTx are excreted from the kidney into urine, urinary concentrations of these substances has been used as the means for estimation of osteoclastic bone resorption [10,32]. The urinary excretion of CTx and DPD was found to be elevated in the diabetic group and to be positively correlated with serum levels of TRAP. These results comfirm that the osteoclastic activity is significantly increased in type 2 diabetic patients.

It has been recognized that OCIF/OPG modifies osteoclastic differentiation by binding to ODF as decoy receptor, and then suppresses the generation of mature osteoclasts from their precurcer cells [33]. In addition, it has been reported that recombinant OCIF/OPG inhibits osteoclastogenesis in a dose-dependent manner in vitro, and increases bone mineral density and bone volume in vivo, associated with a decrease of active osteoclast number in normal rats [34]. In our studies, unexpectedly, the circulating levels of OCIF/OPG tended to be rather increased in type 2 diabetic patients. On the other hand, serum OCIF/OPG exhibited significantly positive correlation with serum TRAP, so that, it is possible that OCIF/OPG plays a protective role against the increased bone resorption under diabetic condition. In addition, a negative correlation between OCIF/OPG and m-BMD might be related to the putative role of this osteoblast-derived cytokine to prevent further loss of the bone mass in diabetic patients.

It has been reported that serum OCIF/OPG is very sensitive to renal function. For example, the age-related increase in serum OCIF/OPG is likely to be related to modest deterioration in glomerular filtration rate with age [35]. We excluded diabetic patients with evident renal dysfunction in this study. Furthermore, there was no significant correlation between serum OCIF/OPG and corrected urine albumin (data not shown). Although it is true that OCIF/OPG is osteoblast-derived, OCIF/OPG has other roles, and the majority of plasma OCIF/OPG is likely to be derived from not only bone but also other various tissues [36]. In particular, OCIF/OPG has been reported to be involved in vascular physiology and its pathology [14]. In our preliminary study, however, no significant difference in serum levels of OCIF/OPG was found among the patients with various stages of diabetic retinopathy or neuropathy (data not shown). It is still unclear whether the etiological background is common in diabetic osteopenia and various kinds of vasculopathy in type 2 diabetic patients, because the examination on those with microvascular and macrovasular complications were not performed in the present study. Further investigation will be needed in order to resolve the relationship between OCIF/OPG and diabetic vasculopathy.

The clinical management of diabetic osteopenia would become important for the preservation of quality of life in older diabetic patients, because it has been recently recognized that metabolic derangement under diabetic condition is related to the risk of bone fracture [37]. Further efforts should be necessary to clarify the detailed underlying mechanism and to establish the preventive methods for osteopenia in diabetic patients.

References

[1] J. Me Levin, C. Vincenza, VC. Boisseau, L.V. Avioli, Effects of diabetes mellitus on bone mass in juvenile and adult-onset diabetes, N. Eng. J. Med. 294 (1976) 241–245.

[2] P. McNair, S. Madsbad, C. Christiansen, O.K. Faber, I. Transbøl, C. Binder, Osteopenia in insulin treated diabetes mellitus. Its relation to age at onset, sex and duration of disease, Diabetologia 15 (1978) 87–90.

[3] H. Ishida, Y. Seino, S. Matsukura, et al. Diabetic osteopenia and circulating levels of vitamin D metabolites in type 2 (noninsulin-dependent) diabetes, Metabolism 34 (1985) 797–801.
[4] Y. Seino, H. Ishida, Diabetic osteopenia: pathophysiology and clinical aspects, Diabetes Metab. Rev. 11 (1995) 21–35.
[5] R. Okazaki, Y. Totsuka, K. Hamano, et al. Metabolic improvement of poorly controlled noninsulin-dependent diabetes mellitus decreases bone turnover, J. Clin. Endocrinol. Metab. 82 (1997) 2915–2970.
[6] K. Suzuki, C. Sugimoto, M. Takizawa, et al. Correlation between bone mineral density and circulating bone metabolic markers in diabetic patients, Diabetes Res. Clin. Pract. 48 (2000) 185–191.
[7] K. Suzuki, Y. Taguchi, H. Ishida, Y. Seino, The evidence for uncoupling between bone formation and resorption in NIDDM patients, Diabetologia 40 (Suppl. 1) (1997) A581.
[8] R. Okazaki, M. Miura, M. Toriumi, et al. Short-term treatment with troglitazone decreases bone turnover in patients with type 2 diabetes mellitus, Endocr. J. 46 (1999) 795–801.
[9] M. Donde, C. Fledelius, P. Qvist, C. Christiansen, Coated-tube radioimmunoassay for C-telopeptides of type I collagen to assess bone resorption, Clin. Chem. 42 (1996) 1639–1644.
[10] D. Unbelhart, A. Schlemmer, J.S. Johansen, E. Gineyts, C. Christiansen, P. Delmas, Effect of menopause and hormone replacement therapy on the urinary excretion of pyridinium cross-links, J. Clin. Endocrinol. Metab. 72 (1991) 367–373.
[11] M.A. Da Hanson, A.M. Weis, S.L. Bollen, F.R. Maslan, D.R. Singer, Eyre Specific immunoassay for monitoring human bone resorption: quantitation of type I collagen cross-linked N-telopeptide in urine, J. Bone Miner. Res. 7 (1992) 1251–1258.
[12] D.M. Anderson, E. Marakovsky, W.L. Billingsley, et al. A homologue of the TNF receptor and its ligand enhance T-cell growth and dendric-cell function, Nature 390 (1997) 175–179.
[13] DL. Lacey, E. Timms, H.L. Tan, et al. Osteoprotegerin ligand is a cytokine that regulates osteoclast differentiation and activation, Cell 93 (1998) 165–176.
[14] E. Tsuda, M. Goto, S. Mochizuki, et al. Isolation of a novel cytokine from human fibroblasts that specifically inhibits osteoclastogenesis, Biochem. Biophys. Res. Commun. 234 (1997) 137–142.
[15] W.S. Browner, L.Y. Lui, S.R. Cummings, Associations of serum osteoprotegerin levels with diabetes, stroke, bone density, fractures, and mortality in elderly women, J. Clin. Endocrinol. Metab. 86 (2001) 631–637.
[16] K. Suzuki, H. Ishida, C. Sugimoto, et al. The urinary concentration of sialic acid is increased in non-insulin-dependent diabetic patients with microangipathy: a possible useful marker for diabetic microangiopathy, Diabetic Med. 12 (1995) 1092–1096.
[17] G. Mundy, R. Garrett, S. Harris, et al. Stimulation of bone formation in vitro and in rodents by statins, Science 286 (1999) 1946–1949.
[18] H. Ishida, K. Suzuki, Y. Someya, et al. Possible compensatory role of parathyroid hormone-related peptide on maintenance of calcium homeostasis in patients with non-insulin dependent diabetes mellitus, Acta Endocrinol. (*Copenhagen*) 129 (1993) 519–524.
[19] K. Nakashima, Y. Hattori, K. Yamazaki, et al. Immediate elimination of labile HbA1c with allosteric effectors of hemoglobin, Diabetes 39 (1990) 17–21.
[20] K. Takai, K. Nanaka, K. Ichihara, et al. Food constituents as a cause of variation of C-peptide excretion in the urine, Endocrinol. Jpn. 31 (1984) 291–299.
[21] K. Hosoda, H. Eguchi, T. Nakamoto, et al. Sandwich immunoassay for intact osteocalcin, Clin. Chem. 38 (1992) 2233–2238.
[22] K. Suzuki, H. Ishida, T. Takeshita, et al. Circulating levels of tartrate-resistant acid phosphatase in rat models of non-insulin-dependent diabetes mellitus, J. Diabetes Comp. 12 (1998) 176–180.
[23] W.D. Fraser, B.H. Durham, J.L. Berry, E.B. Mawer, Measurement of plasma 1, 25 dihydroxyvitamin D using a novel immunoextraction technique and immunoassay with iodine labeled vitamin D tracer, Ann. Clin. Biochem. 34 (1997) 632–637.
[24] PLA. Van Daele, R.P. Stolk, H. Burger, et al. Bone density in non-insulin-dependent diabetes mellitus, Ann. Intern. Med. 122 (1995) 409–414.
[25] J.C. Krakauer, M.J. Mckenna, N.F. Buderer, D.S. Rao, F.W. Whitehouse, A.M. Parfitt, Bone loss and bone turnover in diabetes, Diabetes 44 (1995) 775–782.
[26] S. Hough, L.V. Avioli, M.A. Bergfell, M.D. Fallon, E. Slatopolsky, S.L. Teitelbaum, Correction of abnormal bone and mineral metabolism in chronic streptozotocin-induced diabetes mellitus in the rat by insulin therapy, Endocrinology 108 (1981) 2228–2234.
[27] H. Ishida, Y. Seino, T. Taminato, et al. Circulating levels and bone contents of bone γ-carboxyglutamic acid-containing protein are decreased in streptozotocin-induced diabetic osteopenia, Diabetes 37 (1988) 702–706.
[28] N. Takeshita, H. Ishida, T. Yamamoto, et al. Circulating levels of and bone contents of bone γ-carboxyglutamic acid-containing protein in rat models of noninsulin-dependent diabetes mellitus, Acta Endocrinol. (*Copenhagen*) 128 (1993) 69–73.
[29] J. Verhaegue, A.M. Suiker, T.A. Einhorn, et al. Brittle bones in spontaneously diabetic female rats cannot be predicted by bone mineral measurements: Studies in diabetic and ovariectomized rats, J. Bone Miner. Res. 9 (1994) 1657–1667.
[30] B. Piekorn, P. Kann, T. Forst, J. Andreas, A. Ptűtzner, J. Beyer, Bone mineral density and bone metabolism in diabetes mellitus, Horm. Metab. Res. 29 (1997) 204–219.
[31] C. Fledelius, A.H. Johnsen, P. Cloos, M. Bonde, P. Qvist, Characterization of urinary degradation products derived from type I collagen, J. Biol. Chem. 272 (1997) 9755–9763.
[32] A. Colwell, R.G.G. Russell, R. Eastell, Factors affecting the assay of urinary 3-hydroxypyridinium crosslinks of collagen as markers of bone resorption, Eur. J. Clin. Invest. 23 (1993) 341–349.
[33] H. Yasuda, N. Shima, N. Nakagawa, et al. Osteoclast differentiation factor is a ligand for osteoprotegerin/osteoclastogenesis-inhibitory factor and is identical to TRANCE/RANKL, Proc. Natl. Acad. Sci. U.S.A. 95 (1998) 3597–3602.

[34] H. Yasuda, N. Shima, N. Nakagawa, et al. Identity of osteoclastogenesis inhibitory factor (OCIF) and osteoprotegerin (OPG): a mechanism by which OPG/OCIF inhibits osteoclastogenesis in vitro, Endocrinology 139 (1998) 1329–1337.

[35] JJ. Kazama, T. Shigematsu, K. Yano, et al. Increased circulting levels of osteoclastgenesis inhibitory factor (osteoprotegerin) in patients with chronic renal failure, Am. J. Kidney Dis. 39 (2002) 525–532.

[36] W.S. Simonet, D.L. Lacey, C.R. Dunsta, et al. Osteoprotegrin: a nobel secreted protein involved in the regulation of bone density, Cell 89 (1997) 309–319.

[37] A.V. Schwartz, D.E. Sellmeyer, K.E. Ensrud, et al. Older women with diabetes have an increased risk of fracture; a prospective study, J. Clin. Endocrinol. Metab. 86 (2001) 32–38.

Am J Physiol Endocrinol Metab 289: E643–E649, 2005.
First published May 31, 2005; doi:10.1152/ajpendo.00456.2004.

Activators of AMP-activated protein kinase enhance GLUT4 translocation and its glucose transport activity in 3T3-L1 adipocytes

Shinya Yamaguchi,[1] Hiroshi Katahira,[1] Sachihiko Ozawa,[1] Yoko Nakamichi,[2] Toshiaki Tanaka,[1] Tatsuhiro Shimoyama,[1] Kazuto Takahashi,[1] Katsuhiko Yoshimoto,[1] Mica Ohara Imaizumi,[2] Shinya Nagamatsu,[2] and Hitoshi Ishida[1]

[1]*Third Department of Internal Medicine and* [2]*Department of Biochemistry, Kyorin University, Mitaka, Tokyo, Japan*

Submitted 27 October 2004; accepted in final form 5 May 2005

Yamaguchi, Shinya, Hiroshi Katahira, Sachihiko Ozawa, Yoko Nakamichi, Toshiaki Tanaka, Tatsuhiro Shimoyama, Kazuto Takahashi, Katsuhiko Yoshimoto, Mica Ohara Imaizumi, Shinya Nagamatsu, and Hitoshi Ishida. Activators of AMP-activated protein kinase enhance GLUT4 translocation and its glucose transport activity in 3T3-L1 adipocytes. *Am J Physiol Endocrinol Metab* 289: E643–E649, 2005. First published May 31, 2005; doi:10.1152/ajpendo.00456.2004.—To determine whether the increase in glucose uptake following AMP-activated protein kinase (AMPK) activation in adipocytes is mediated by accelerated GLUT4 translocation into plasma membrane, we constructed a chimera between GLUT4 and enhanced green fluorescent protein (GLUT4-eGFP) and transferred its cDNA into the nucleus of 3T3-L1 adipocytes. Then, the dynamics of GLUT4-eGFP translocation were visualized in living cells by means of laser scanning confocal microscopy. It was revealed that the stimulation with 5-aminoimidazole-4-carboxamide-1-β-D-ribofuranoside (AICAR) and 2,4-dinitrophenol (DNP), known activators of AMPK, promptly accelerates its translocation within 4 min, as was found in the case of insulin stimulation. The insulin-induced GLUT4 translocation was markedly inhibited after addition of wortmannin ($P < 0.01$). However, the GLUT4 translocation through AMPK activators AICAR and DNP was not affected by wortmannin. Insulin- and AMPK-activated translocation of GLUT4 was not inhibited by SB-203580, an inhibitor of p38 mitogen-activated protein kinase (MAPK). Glucose uptake was significantly increased after addition of AMPK activators AICAR and DNP ($P < 0.05$). AMPK- and insulin-stimulated glucose uptake were similarly suppressed by wortmannin ($P < 0.05$–0.01). In addition, SB-203580 also significantly prevented the enhancement of glucose uptake induced by AMPK and insulin ($P < 0.05$). These results suggest that AMPK-activated GLUT4 translocation in 3T3-L1 adipocytes is mediated through the insulin-signaling pathway distal to the site of activated phosphatidylinositol 3-kinase or through a signaling system distinct from that activated by insulin. On the other hand, the increase of glucose uptake dependent on AMPK activators AICAR and DNP would be additionally due to enhancement of the intrinsic activity in translocated GLUT4 protein, possibly through a p38 MAPK-dependent mechanism.

glucose transporter 4; mitogen-activated protein kinase; phosphatidylinositol 3-kinase; enhanced green fluorescent protein

IT HAS BEEN ESTABLISHED that insulin-stimulated glucose uptake into adipocytes and skeletal myocytes involves the translocation of GLUT4 from an intracellular pool to the plasma membrane. The intracellular mechanism for the recruitment of GLUT4-containing vesicle into plasma membrane has been investigated, and it has been revealed that phosphatidylinositol 3-kinase (PI3K) plays a crucial role in insulin-stimulated GLUT4 translocation (7, 14, 24). However, little has been elucidated concerning other mechanisms to enhance the GLUT4 translocation than the insulin signaling system.

AMP-activated protein kinases (AMPKs) have been known to act as a metabolic sensor in mammalian cells (9, 30). The kinase activity is enhanced by a relative increase in cellular AMP level (increase in AMP-to-ATP ratio) through a metabolic uncoupler, dinitrophenol (DNP), to decrease ATP concentration and by 5-aminoimidazole-4-carboxamide-1-β-D-ribofuranoside (AICAR), an adenosine analog. After entering into cells, AICAR is phosphorylated, and the reaction product 5-aminoimidazole-4-carboxamide ribonucleotide mimics the action of AMP to activate AMPK (6, 19). In the case of skeletal myocytes, activation of AMPK through physiological stimulation such as muscle contraction or by the pharmacological activator AICAR leads to a significant increase of glucose uptake mediated by the translocation of GLUT4 (10, 20).

It has been reported that GLUT4 translocation is accelerated by stimulation other than by insulin, such as hyperosmolar shock and bradykinin (2, 4, 15), but the precise mechanism has not yet been elucidated. In addition, although AMPK activation by AICAR in adipocytes has also been observed to increase glucose uptake under basal conditions (27), it seems to be still unclear whether or not its increase is mediated by GLUT4 translocation. In this study, we monitored in real time the GLUT4 trafficking in living, single 3T3-L1 adipocytes by use of a chimera between GLUT4 and the intrinsically fluorescent enhanced green fluorescent protein (eGFP). The time-dependent acceleration of GLUT4 translocation was measured using laser-scanning confocal microscopy after AMPK activation by AICAR and DNP. The effect of insulin was examined in parallel for a comparative purpose. The involvement of PI3K and p38 mitogen-activated protein kinase (MAPK) activation was also investigated in the mechanisms for accelerated GLUT4 translocation and increased glucose uptake through AMPK activation in 3T3-L1 adipocytes.

MATERIALS AND METHODS

Materials. Wortmannin, AICAR, and bovine serum albumin (BSA) were from Sigma (St. Louis, MO), and DNP and 2-deoxy-D-glucose (2-DG) were from Wako (Osaka, Japan). SB-203850 was from Calbiochem (La Jolla, CA). 2-[^{14}C]DG (300 mCi/mmol) was obtained from DuPont-NEN (Boston, MA). Human GLUT4 cDNA was a generous gift from Dr. G. I. Bell (University of Chicago). The GLUT4-eGFP construct was prepared by subcloning the full-length GLUT4 cDNA in frame into the *Hin*dIII and *Eco*R1 sites of the peGFP vector (Clontech, Palo Alto, CA) to make a COOH-terminal eGFP fusion.

Address for reprint requests and other correspondence: H. Ishida, Kyorin Univ. School of Medicine, 6-20-2 Shinkawa, Mitaka, Tokyo 181-8611, Japan (e-mail: ishida@kyorin-u.ac.jp).

The costs of publication of this article were defrayed in part by the payment of page charges. The article must therefore be hereby marked "*advertisement*" in accordance with 18 U.S.C. Section 1734 solely to indicate this fact.

Preparation of cells. 3T3-L1 cells were obtained from the cell bank of Japanese Collection of Research Bioresouces (Tokyo, Japan). Cells were seeded and fed every 2–3 days in Dulbecco's modified Eagle's medium (DMEM) high glucose supplemented with 50 U/ml penicillin, 50 μg/ml streptomycin, 100 mM MEM sodium pyruvate, and 10% fetal calf serum and were grown under 5% CO_2 at 37°C. At confluence, differentiation was started by addition of medium containing 500 μM isobutylmethylxanthine (IBMX, Sigma), 250 μM dexamethasone (Sigma), and 1.7 μM insulin. After 48 h, this mixture was replaced with fresh medium. Between *days 7* and *10* after induction of differentiation, the glucose uptake was determined using 2-[^{14}C]DG, and the dynamics of GLUT4 translocation were monitored in living cells by transferring the cDNA of GLUT4-eGFP into their nucleus.

Cell microinjection of GLUT4-eGFP cDNA. 3T3-L1 adipocytes were injected with cDNA of GLUT4-eGFP using an Eppendorf microinjector system (Femtojet; Eppendorf, Hamburg, Germany) fit-

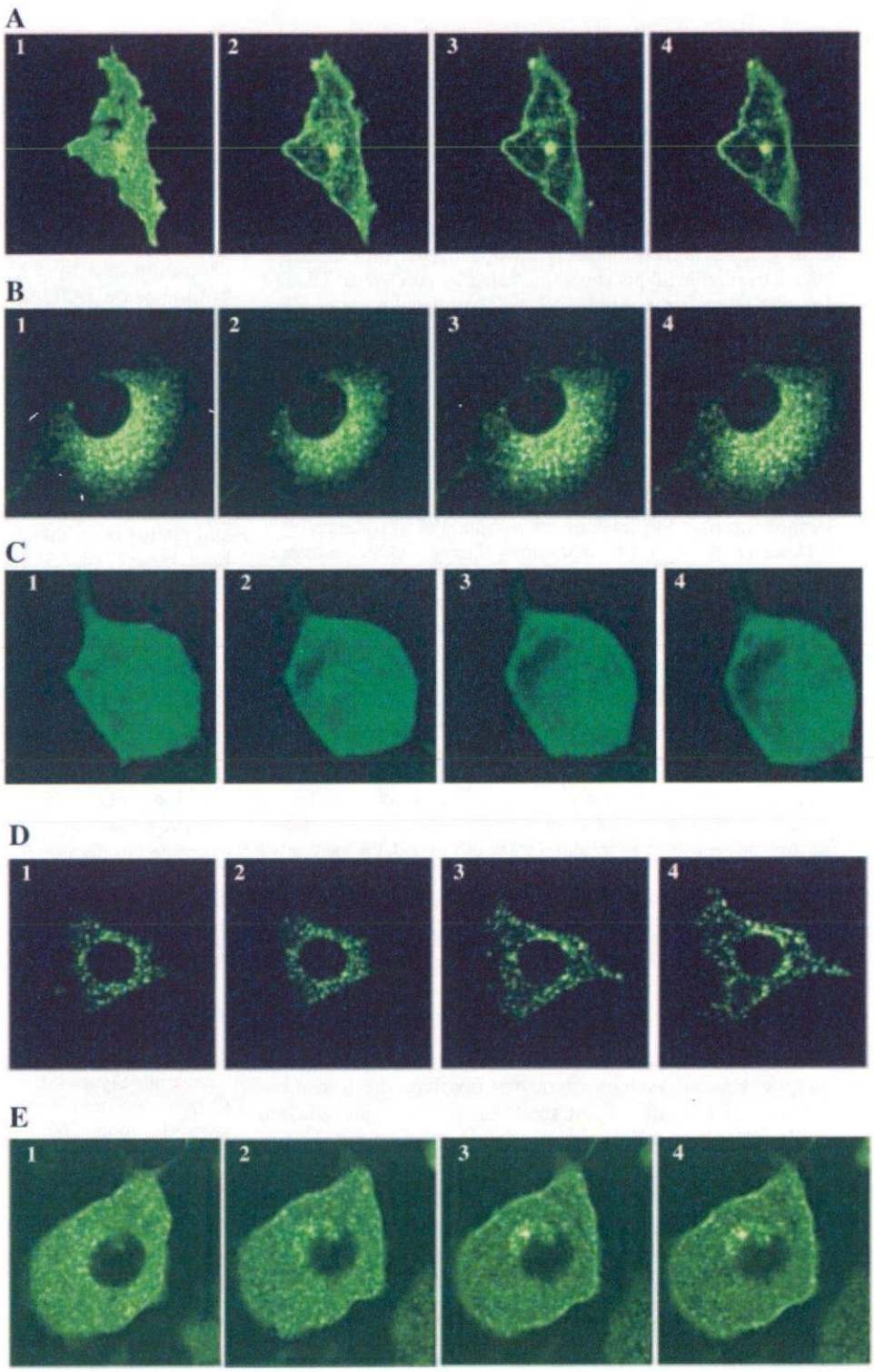

Fig. 1. Visualization of GLUT4 translocation using GLUT4-eGFP (enhanced green fluorescent protein) chimeric protein and dynamics of its intracellular distribution after addition of stimulants. Each image was obtained using laser-scanning confocal microscopy before (*1*), and 4 (*2*), 10 (*3*), and 20 min (*4*) after the following stimulations: *A*: 10^{-7} M insulin alone; *B*: 10^{-7} M insulin + 3×10^{-8} M wortmannin; *C*: 10^{-7} M insulin + 10^{-5} M SB-203580 (an inhibitor of p38 MAPK); *D*: 10^{-4} M 2,4-dinitrophenol (DNP) alone; *E*: 10^{-4} M DNP + 3×10^{-8} M wortmannin.

ted on to Zeiss Axiovert microscope. In each coverslip, the plasmid of GLUT4-eGFP cDNA adjusted to 50–200 μg/ml in 10 mM Tris·HCl buffer (pH 8.0) plus 1 mM EDTA was injected into the nucleus of ~50 cells. After injection, cells were washed twice with DMEM containing 10% fetal calf serum and incubated for 16–24 h under 5% CO_2 at 37°C. The efficiency of gene transfer into cells was in the range of 8–27%.

Experimental protocol for stimulation with insulin, DNP, or AICAR. After the preincubation of differentiated 3T3-L1 adipocytes in Krebs-Ringer bicarbonate (KRB) buffer containing (in mM) 110 NaCl, 4.4 KCl, 1.45 KH_2PO_4, 1.2 $MgCl_2$, 2.3 calcium gluconate, 4.8 $NaHCO_3$, 11 glucose, and 10 HEPES (pH 7.4) and 0.3% BSA (for GLUT4 translocation) or in serum-free Hanks' buffer (in mM: 136.9 NaCl, 5.6 KCl, 0.34 $Na_2HPO_4 \cdot 7H_2O$, 0.44 KH_2PO_4, 1.27 $CaCl_2$, and 4.2 $NaHCO_3$ and 0.02% BSA, pH 7.4) (for 2-DG uptake) at 37°C for 140 min, cells were then additionally incubated with 10^{-7} M insulin, 10^{-4} M DNP or 10^{-3} M AICAR for 20 min. In experiments where the PI3K inhibitor (3×10^{-8} M wortmannin) or the p38 MAPK inhibitor (10^{-5} M SB-203085) was used, each agent was added to the buffer 20 min before the addition of insulin, DNP, or AICAR.

Image capture of GLUT4 translocation and its analysis. The transfected 3T3-L1 adipocytes with GLUT4-eGFP were imaged with a laser-scanning confocal microscope LSM 510 (Carl Zeiss, Jena, Germany) to monitor the dynamics of GLUT4 translocation. Transfected cells were on a heated stage adjusted to provide a temperature of 37°C in the bathing KRB buffer. Images were collected using 488-nm excitation wavelength every 1 min. The eGFP signals were analyzed with NIH Image software (version 1.61, National Institute of Mental Health, NIMH Public Inquiries, Bethesda, MD). To quantify the extent of GLUT4-eGFP translocation to the plasma membrane, the ratio of fluorescence intensity in the peripheral region to that in the remaining cellular fluorescence was calculated. The peripheral-to-cellular ratio in the basal state was expressed as 100(%), and the area under the curve during the 20-min stimulation was calculated for the quantitative comparison.

2-DG uptake assay. The differentiated 3T3-L1 adipocytes were serum starved using serum-free Hanks' buffer (pH 7.4) prior to glucose uptake experiments, as described above, and were preincubated for 140 min. For 2-DG uptake measurements, 0.2 μCi 2-[^{14}C]DG was then added to the medium containing 1 mM nonra-

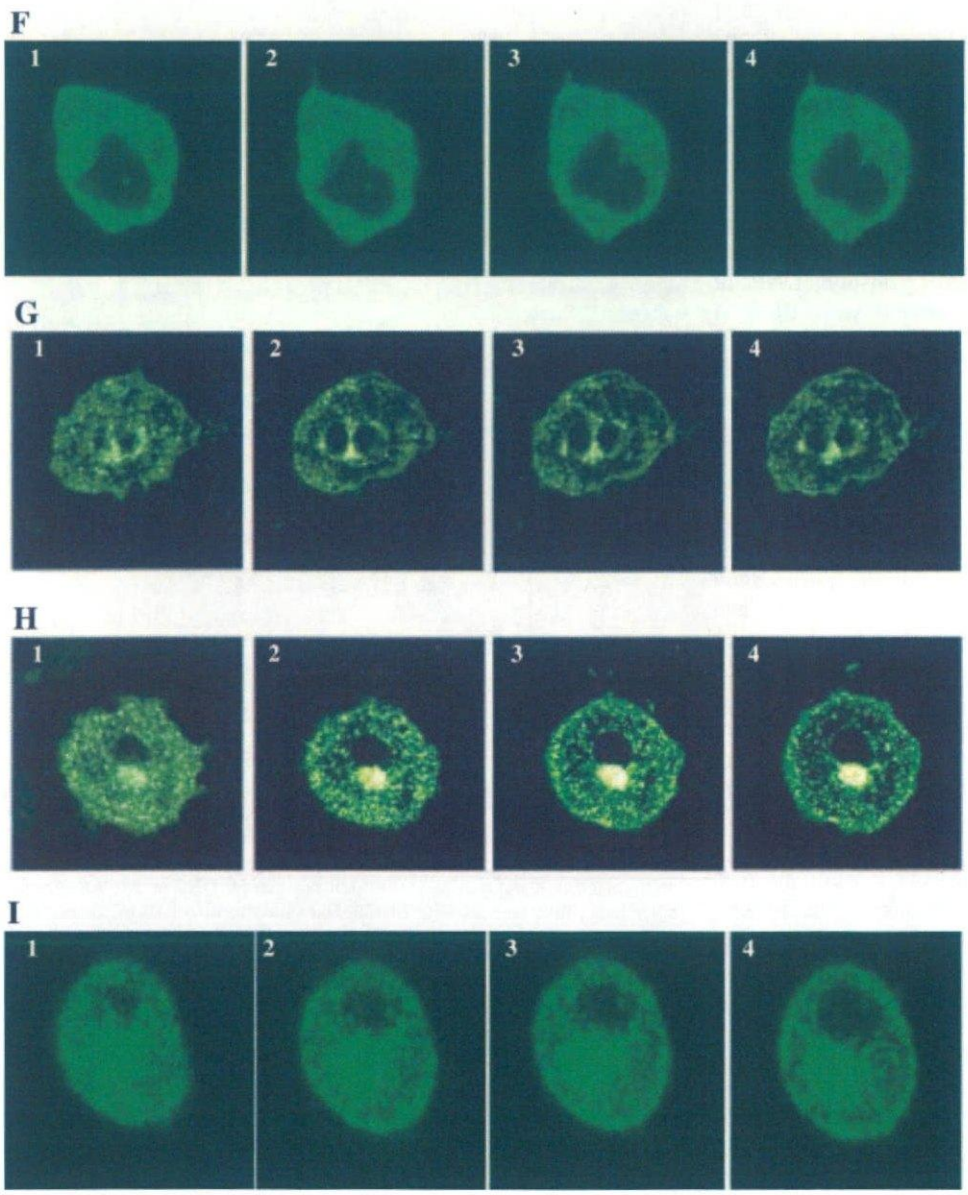

Fig. 1. *F*: 10^{-4} M DNP + 10^{-5} M SB-203580; *G*: 10^{-3} M 5-aminoimidazole-4-carboxamide-1-β-D-ribofuranoside (AICAR) alone; *H*: 10^{-3} M AICAR + 3×10^{-8} M wortmannin; *I*: 10^{-3} M AICAR + 10^{-5} M SB-203580.

dioactive 2-DG. After the incubation for 20 min at room temperature along with each stimulant (insulin, DNP, or AICAR), glucose uptake was stopped by aspiration of the buffer. Cells were rapidly washed several times with 1 ml of ice-cold phosphate-buffered saline and solubilized by the addition of 0.2 M NaOH. Nonspecific uptake was determined in parallel in the presence of 10 μM cytochalasin B. The radioactivity associated with the cells was measured using a scintillation counter (LSC-3100; Aloca, Tokyo, Japan), as has been described previously (21).

Statistical analysis. Statistical analysis was performed by analysis of variance using StatView computer software (Abacus, Berkeley, CA). Results are expressed as means ± SE, and $P < 0.05$ was considered significant.

RESULTS

Visualization of GLUT4 translocation and its dynamics of intracellular distribution. The dynamics of GLUT4-eGFP translocation were visualized and monitored using laser-scanning confocal microscopy. Each image in Fig. 1 indicates the intracellular localization of GLUT4 before (1), and 4 (2), 10 (3), and 20 min (4) after the addition of 10^{-7} M insulin, 10^{-4} MDNP, or 10^{-3} M AICAR. As indicated in Fig. 1*A*, insulin stimulation elicited GLUT4 translocation into plasma membrane within 4 min. On the other hand, the time-dependent translocation was almost diminished by the pretreatment with 3×10^{-8} M wortmannin (Fig. 1*B*). Administration of DNP or AICAR alone similarly promoted GLUT4 translocation within 4 min in a time-dependent manner (Fig. 1, *D* and *G*). The pretreatment with wortmannin, however, failed to inhibit the translocation by DNP or AICAR (Fig. 1, *E* and *H*). In addition, the translocation induced by insulin, DNP, or AICAR was not affected by the pretreatment with 10^{-5} M SB-203580. (Fig. 1, *C, F,* and *I*).

Quantitative assessment of GLUT4 translocation by each stimulant. A significant increase in the peripheral/cellular ratio of GLUT4-eGFP fluorescence intensity was observed 4 min after the addition of insulin (138.2 ± 13.3% of the basal state, $P < 0.05$), and it consistently continued thereafter ($P < 0.05$; Fig. 2*A*). When the cells were pretreated with wortmannin, however, no apparent acceleration of the GLUT4 translocation was found, and the statistically significant suppression was noted in the translocation during the insulin stimulation ($P < 0.05$; Fig. 2*A*). DNP and AICAR also significantly enhanced the GLUT4 translocation 4 min after the addition (140 ± 10.5 and 130.7 ± 8.5% of the basal state in DNP and AICAR stimulation, respectively, $P < 0.05$; Fig. 2, *B* and *C*). In contrast, the wortmannin pretreatment failed to suppress the GLUT4 translocation stimulated with DNP or AICAR (Fig. 2, *B* and *C*). The addition of SB-203580 did not suppress the translocation by insulin, DNP or AICAR (Fig. 2, *A–C*). When the area under the curve of peripheral/cellular ratio of fluorescence intensity was calculated (Fig. 3*A*), it was confirmed that wortmannin could almost completely inhibit the insulin-induced GLUT4 translocation (63,081 ± 8,516 and 181 ± 844 arbitary units in insulin alone and insulin plus wortmannin, respectively, $P < 0.01$), but not by DNP or AICAR (Fig. 3, *B* and *C*). No significant effect on the accelerated translocation by insulin, DNP, or AICAR was observed by the addition of SB-203580 (Fig. 3, *A–C*).

Insulin-, DNP-, and AICAR-induced 2-DG uptake inhibition by wortmannin or SB-203580. The stimulation by insulin, DNP, and AICAR enhanced 2-DG uptake 2.8 ± 0.14-, 2.4 ± 0.21-, and 1.7 ± 0.14-fold, respectively ($P < 0.01$). The addition of wortmannin did not affect the basal 2-DG uptake but markedly suppressed the insulin-induced glucose uptake (5,215 ± 429 and 1,618 ± 277 cpm/10^6 cells in insulin alone and insulin plus wortmannin, respectively, $P < 0.01$). Inter-

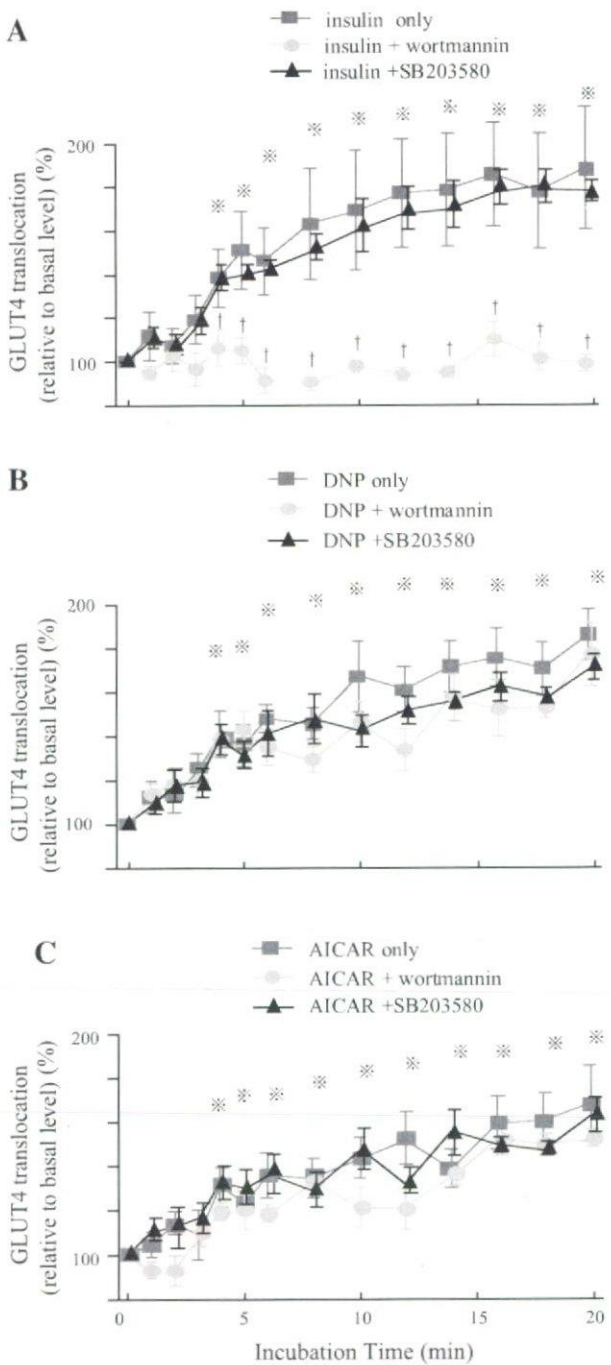

Fig. 2. Time course of quantified GLUT4 translocation in 3T3-L1 adipocytes after addition of 10^{-7} M insulin (*A*), 10^{-4} M DNP (*B*), and 10^{-3} M AICAR (*C*). These agents similarly elicited a significant increase of GLUT4 translocation 4 min after their addition. Wortmannin pretreatment markedly reduced the translocation induced by insulin but not that by DNP or AICAR. On the other hand, pretreatment with SB-203580 failed to affect all of them. *$P <$ 0.05 vs. nonstimulatory basal condition. †$P < 0.05$ vs. corresponding control. Data are means ± SE of 6 determinations on different 3T3-L1 cells.

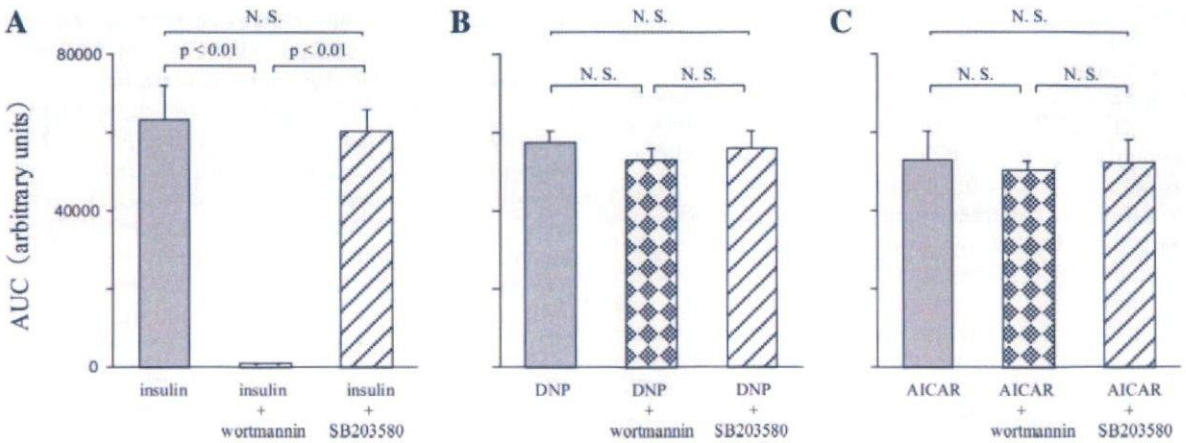

Fig. 3. Calculation of area under the curve (AUC) of %peripheral/cellular ratio of GLUT4-eGFP fluorescence intensity after addition of 10^{-7} M insulin (*A*), 10^{-4} M DNP (*B*), and 10^{-3} M AICAR (*C*). Accelerated GLUT4 translocation by insulin was significantly suppressed by 3×10^{-8} M wortmannin ($P < 0.01$) but not by 10^{-5} M SB-203580. DNP- or AICAR-induced GLUT4 translocation was not affected by these agents. N.S., not significant. Data are means ± SE of 6 determinations on different 3T3-L1 cells.

estingly, wortmannin treatment could also significantly inhibit 2-DG uptake by DNP and AICAR (4,625 ± 555 and 2,903 ± 65 cpm/10^6 cells in DNP alone and DNP plus wortmannin, respectively, $P < 0.05$, and 3,140 ± 381 and 1,891 ± 150 cpm/10^6 cells in AICAR alone and AICAR plus wortmannin, respectively, $P < 0.05$; Fig. 4*A*), whereas wortmannin failed to suppress the GLUT4 translocation stimulated by these agents, as has been described above. In another series of experiments, SB-203580 pretreatment was found to significantly inhibit the glucose uptake enhanced by insulin (5,752 ± 190 and 3,692 ± 67 cpm/10^6 cells in insulin alone and insulin plus SB-203580, respectively, $P < 0.05$) and also by DNP and AICAR (4,062 ± 212 and 3,072 ± 168 cpm/10^6 cells in DNP alone and DNP plus SB-203580, respectively, $P < 0.05$; 4,880 ± 316 and 2,444 ± 99 cpm/10^6 cells in AICAR alone and AICAR plus SB-203580, respectively, $P < 0.05$; Fig. 4*B*).

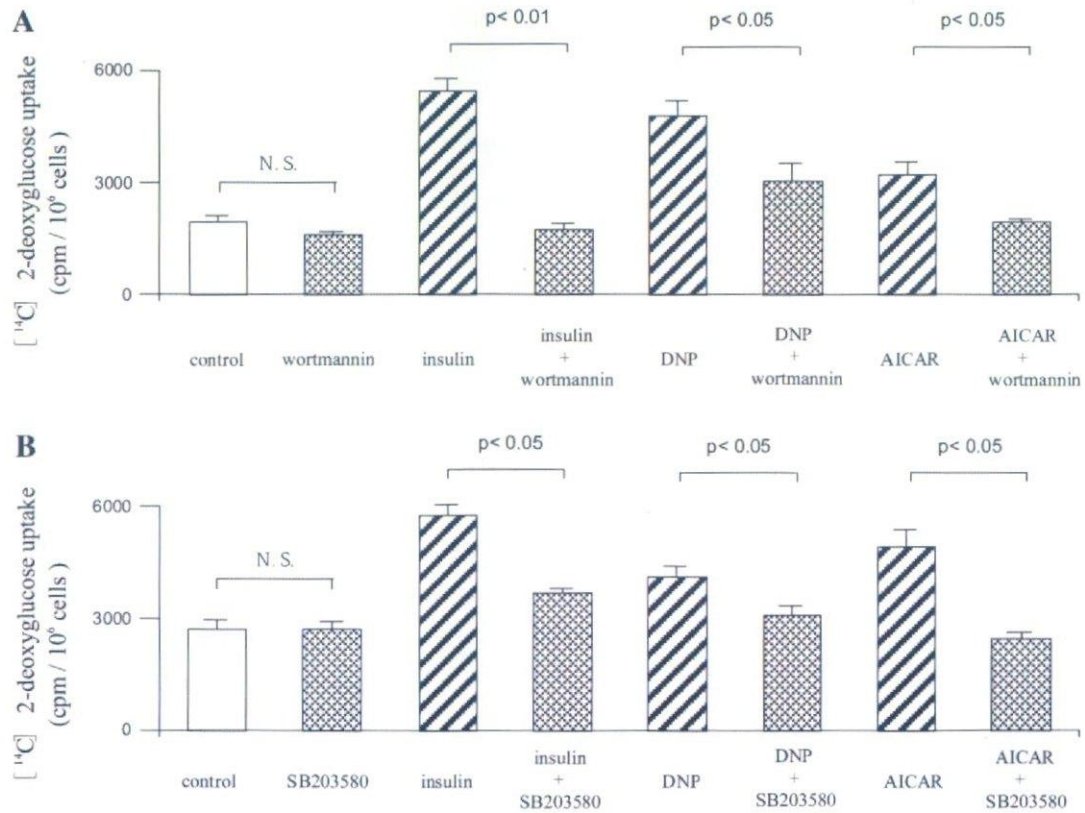

Fig. 4. Stimulation of glucose transport activity in 3T3-L1 adipocytes by insulin, DNP, and AICAR and its suppression by wortmannin (*A*) and SB-203580 (*B*). *A*: addition of wortmannin significantly reduced the glucose uptake stimulated by insulin, as well as that evoked by DNP and AICAR ($P < 0.05$–0.01). *B*: enhanced glucose uptakes by insulin, DNP, and AICAR were all significantly suppressed by addition of SB-203580 ($P < 0.05$). Data are means ± SE of 6 determinations.

DISCUSSION

Through the monitoring system of visualized GLUT4-eGFP translocation (22, 25), we have demonstrated here that the stimulation with DNP and AICAR, known activators of AMPK, promptly promotes the GLUT4 translocation within 4 min, as has been previously reported in the case of insulin (13, 16, 23). In addition, the translocation induced by DNP and AICAR was not affected by wortmannin, suggesting that AMPK-stimulated GLUT4 translocation in 3T3-L1 adipocytes is mediated through the insulin-signaling pathway distal to the site of activated PI3K or through a signaling system distinct from that of insulin. This finding seems to be consistent with the case of enhanced GLUT4 translocation in skeletal muscles, in which AMPK activity has reportedly been elevated through their contraction (11, 17). Because the GLUT4 translocation induced by insulin stimulation and AMPK activation in 3T3-L1 adipocytes was not found to be affected by SB-203580, a known inhibitor of p38 MAPK, the recruitment of GLUT4 to the plasma membrane was unlikely to have been mediated by p38 MAPK signaling.

The addition of AMPK activators AICAR and DNP enhanced glucose uptake in 3T3-L1 adipocytes, as was found in the case of insulin stimulation. In contrast to the case of GLUT4 translocation, however, the glucose transport activity was significantly reduced by the addition of wortmannin. It has been supposed that the magnitude of glucose transport after insulin stimulation is regulated by promoting the GLUT4 translocation via PI3K activation (7, 14, 24) and also through increasing the intrinsic transport activity of GLUT4 by protein phosphorylation via p38 MAPK activation (3, 28, 29). Although wortmannin has been used as an inhibitor of PI3K, this agent has been additionally reported to inhibit insulin-dependent p38α and p38β MAPK activities with an IC_{50} of 6×10^{-9} M and 2×10^{-9} M, respectively (28). Because the concentration of wortmannin used in this experiment was 3×10^{-8} M, it can be expected that it suppresses the p38 MAPK activities in 3T3-L1 adipocytes. In fact, the AMPK-activated glucose transport activity was found to be significantly suppressed by SB-203580 in the present study. Because the magnitude of the 2-DG transport response by insulin and AMPK activators was found to be relatively poor compared with that in previous studies (3, 29), the degree of cell differentiation of 3T3-L1 adipocytes might have been lower in our cell preparations. However, the significance in the reduction of glucose uptake by the addition of wortmannin and SB-203580 could still be valid, because apparent GLUT4 translocation into the plasma membrane of 3T3-L1 adipocytes was observed in the cell preparations similar to those in the glucose uptake assay. It could, accordingly, be speculated that the enhancement of glucose transport induced by AMPK activation in 3T3-L1 adipocytes is mediated by the increase of intrinsic activity through p38 MAPK activation of translocated GLUT4 protein, as has been suggested in the case of skeletal muscle (18). A detailed evaluation would be needed in the future regarding which isoforms of p38α and p38β MAPK can be phosphorylated and activated during this process. However, because it has been demonstrated that SB-203580 inhibited the nucleotide transport system and therefore can indirectly reduce AICAR-stimulated AMPK activity (8), further examinations should be carefully conducted on the exact role of AMPK and p38 MAPK activation in the accelerated glucose uptake activity of GLUT4 protein in 3T3-L1 adipocytes. It has been recently reported that AICAR-stimulated glucose transport was dependent on activation of the extracellular signal-regulated kinase pathway, phospholipase D, and atypical protein kinase C isoforms in myocytes (5). Interestingly, the possible involvement of AMPK-independent signaling has been also proposed, using the system of overexpression of a dominant negative AMPK mutant (26). It should be an interesting issue to be resolved, therefore, how AMPK-dependent and -independent pathways are related to the AICAR-induced glucose uptake observed in 3T3-L1 adipocytes. On the other hand, in adipose cells including 3T3-L1, it has been observed that GLUT1, another isoform of glucose transporters, is also functionally expressed (12). AICAR has been reported to increase the intrinsic activity of GLUT1 protein via activated p38 MAPK to enhance the glucose transport into Clone 9 cells, a rat liver-derived, nontransformed cell line that expresses only the GLUT1 (1, 31). The increased intrinsic activity of GLUT1 as well as GLUT4 could potentially induce the enhancement of glucose uptake after AMPK activation in 3T3-L1 adipocytes. In contrast to our findings, Salt et al. (27) have demonstrated that AICAR does not significantly enhance the translocation of GLUT4 or GLUT1 to the plasma membrane, whereas a modest stimulation of glucose uptake was simultaneously observed. The precise reason for the discrepancy in the translocation of GLUT4 between their results and ours is still unclear at present, but the effect on 3T3-L1 cells might have been too small in their experiments to be detected by the plasma membrane lawn assay, because their method is supposedly less sensitive for the detection compared with ours using the system of the $GLUT_{4\text{-}e}$ GFP chimeric protein. Further studies concerning the intracellular system for translocation and activation of various GLUT isoforms are necessary to clarify this issue.

In the present study, it is revealed that AMPK activators AICAR and DNP can accelerate GLUT4 translocation in 3T3-L1 adipocytes, as has been observed in skeletal muscles. The mode of action on the translocation through AMPK activation was as quick, within 4 min, as in the case of insulin stimulation, but it was shown to be mediated by a signaling system distal to the PI3K activation through insulin stimulation or by a pathway distinct from that activated by insulin. On the other hand, the enhancement of glucose uptake was further mediated by the increased intrinsic activity of GLUT4 protein, possibly through p38 MAPK activation. The activation of AMPK in adipocytes would be a new therapeutic target for the glycemic control of type 2 diabetes.

ACKNOWLEDGMENTS

We are grateful to M. Matsumoto and M. Mase for secretarial work.

GRANTS

This study was supported by Grants-in-Aid for Scientific Research from the Ministry of Education, Science and Culture (to H. Ishida) and by a grant from the Japan Private School Promotion Foundation.

REFERENCES

1. **Abbud W, Habinowski S, Zhang JZ, Kendrew J, Elkairi FS, Kemp BE, Witters LA, and Ismail-Beigi F.** Stimulation of AMP-activated protein kinase (AMPK) is associated with enhancement of GLUT1-mediated glucose transport. *Arch Biochem Biophys* 380: 347–352, 2000.

2. **Barros LF, Barnes K, Ingram JC, Castro J, Porras OH, and Baldwin SA.** Hyperosmotic shock induces both activation and translocation of glucose transporters in mammalian cells. *Pflügers Arch* 442: 614–621, 2001.
3. **Bazuine M, Ouwens DM, Gomes de Mesquita DS, and Massen JA.** Arsenite stimulated glucose transport in 3T3-L1 adipocytes involves both Glut4 translocation and p38 MAPK activity. *Eur J Biochem* 270: 3891–3903, 2003.
4. **Chen D, Elmendorf JS, Olson AL, Li X, Earp HS, and Pessin JE.** Osmotic shock stimulates GLUT4 translocation in 3T3-L1 adipocytes by a novel tyrosine kinase pathway. *J Biol Chem* 272: 27401–27410, 1997.
5. **Chen HC, Bandyopadhyay G, Sajan MP, Kanoh Y, Standaert M, Farese RV Jr, and Farese RV.** Activation of the ERK pathway and atypical protein kinase C isoforms in exercise- and aminoimidazole-4-carboxamide-1-β-D-riboside (AICAR)-stimulated glucose transport. *J Biol Chem* 277: 23554–23562, 2002.
6. **Corton JM, Gillespie JG, Hawley SA, and Hardie DG.** 5-Aminoimidazole-4-carboxamide ribonucleoside: a specific method for activating AMP-activated protein kinase in intact cell? *Eur J Biochem* 229: 558–565, 1995.
7. **Frevert EU and Kahn BB.** Differential effects of constitutively active phosphatidylinositol 3-kinase on glucose transport, glycogen synthase activity and DNA synthesis in 3T3-L1 adipocytes. *Mol Cell Biol* 17: 190–198, 1997.
8. **Fryer LG, Parbu-Patel A, and Carling D.** Protein kinase inhibitors block the stimulation of the AMP-activated protein kinase by 5-amino-4-imidazolecarboxamide riboside. *FEBS Lett* 531: 189–192, 2002.
9. **Hardie DG and Carling D.** The AMP-activated protein kinase: fuel gauge of the mammalian cell? *Eur J Biochem* 246: 259–273, 1997.
10. **Hayashi T, Hirshman MF, Kurth EJ, Winder WW, and Goodyear LJ.** Evidence of 5′ AMP-activated protein kinase mediation of the effect of muscle contraction on glucose transport. *Diabetes* 47: 1369–1373, 1998.
11. **Ihlemann J, Ploug T, Hellsten Y, and Galbo H.** Effect of tension on contraction-induced glucose transport in rat skeletal muscle. *Am J Physiol Endocrinol Metab* 277: E208–E214, 1999.
12. **Kaestner KH, Chirsty RJ, McLenithan JC, Braiterman LT, Cornelius P, Pekala PH, and Lane MD.** Sequence, tissue distribution, and differential expression of mRNA for a putative insulin-responsive glucose transporter in mouse 3T3–L1 adipocytes. *Proc Natl Acad Sci USA* 86: 3150–3154, 1989.
13. **Kanai F, Ito K, Todaka M, Hayashi H, Kamohara S, Ishii K, Okada T, Hazeki O, Ui M, and Ebina Y.** Insulin-stimulated GLUT4 translocation is relevant to the phosphorylation of IRS-1 and the activity of PI3-kinase. *Biochem Biophys Res Commun* 195: 762–768, 1993.
14. **Katagiri H, Asano T, Ishihara H, Inukai K, Shibasaki Y, Kikuchi M, Yazaki Y, and Oka Y.** Overexpression of catalytic subunit p110α of phosphatidylinositol 3-kinase increases glucose transport activity with translocation of glucose transporters in 3T3-L1 adipocytes. *J Biol Chem* 271: 16987–16990, 1996.
15. **Kishi K, Muromoto N, Nakaya Y, Miyata I, Hagi A, Hayashi H, and Ebina Y.** Bradykinin directly triggers GLUT4 translocation via an insulin-independent pathway. *Diabetes* 47: 550–558, 1998.
16. **Kotani K, Carozzi AJ, Sakaue H, Hara K, Robinson LJ, Clark SF, Yonezawa K, James DE, and Kasuga M.** Requirement for phosphoinositide 3-kinase in insulin-stimulated GLUT4 translocation in 3T3-L1 adipocytes. *Biochem Biophys Res Commun* 209: 343–348, 1995.
17. **Kurth-Kraczek EJ, Hirshman MF, Goodyear LJ, and Winder WW.** 5′AMP-activated protein kinase activation causes GLUT4 translocation in skeletal muscle. *Diabetes* 48: 1667–1671, 1999.
18. **Lemieux K, Konrad D, Klip A, and Marette A.** The AMP-activated protein kinase activator AICAR dose not induce GLUT4 translocation to transverse tubules but stimulates glucose uptake and p38 mitogen-activated protein kinases α and β in skeletal muscle. *FASEB J* 17: 1658–1665, 2003.
19. **Merrill GF, Kurth EJ, Hardie DG, and Winder WW.** AICA riboside increases AMP-activated protein kinase, fatty acid oxidation, and glucose uptake in rat muscle. *Am J Physiol Endocrinol Metab* 273: E1107–E1112, 1997.
20. **Mu J, Brozinick JT, Valladares O, Bucan M, and Birnbaum MJ.** A role for AMP-activated protein kinase in contraction- and hypoxia-regulated glucose transport in skeletal muscle. *Mol Cell* 7: 1085–1094, 2001.
21. **Nakamichi Y, Ohara-imaizumi M, Ishida H, and Nagamatsu S.** An insulin-related peptide expressed in 3T3-L1 adipocytes is localized in GLUT4 vesicles and secreted in response to exogenous insulin, which augments the insulin-stimulated glucose uptake. *J Cell Sci* 116: 73–79, 2003.
22. **Oatey PB, Van Weering DHJ, Dobson SP, Gould GW, and Tavaré JM.** GLUT4 vesicle dynamics in 3T3-L1 adipocytes visualized with green-fluorescent protein. *Biochem J* 327: 637–642, 1997.
23. **Patki V, Buxton J, Chawla A, Lifshitz L, Fogarty K, Carrington W, Tuft R, and Corvera S.** Insulin action on GLUT4 traffic visualized in single 3T3-L1 adipocytes by using ultra-fast microscopy. *Mol Biol Cell* 12: 129–141, 2001.
24. **Pessin JE, Thurmond DC, Elmendorf JS, Coker KJ, and Okada S.** Molecular basis of insulin-stimulated GLUT4 vesicle trafficking. *J Biol Chem* 274: 2593–2596, 1999.
25. **Powell KA, Campbell LC, Tavaré JM, Leader DP, Wakefield JA, and Gould GW.** Trafficking of GLUT4-green fluorescent protein chimaeras in 3T3-L1 adipocytes suggests distinct internalization mechamisms regulating cell surface GLUT4 levels. *Biochem J* 344: 535–543, 1999.
26. **Sakoda H, Ogihara T, Anai M, Fujishiro M, Ono H, Onishi Y, Katagiri H, Abe M, Fukushima Y, Shojima N, Inukai K, Kikuchi M, Oka Y, and Asano T.** Activation of AMPK is essential for AICAR-induced glucose uptake by skeletal muscle but not adipocytes. *Am J Physiol Endocrinol Metab* 282: E1239–E1244, 2002.
27. **Salt IP, Connell JMC, and Gould GW.** 5-Aminoimidazole-4-carboxamide ribonucleoside (AICAR) inhibits insulin-stimulated glucose transport in 3T3-L1 adipocytes. *Diabetes* 49: 1649–1656, 2000.
28. **Somwar R, Niu W, Kim DY, Sweeney G, Randhara VK, Huang C, Ramlal T, and Klip A.** Differential effects of phosphatidylinositol 3-kinase inhibition on intracellular signals regulating GLUT4 translocation and glucose transport. *J Biol Chem* 276: 46079–46087, 2001.
29. **Somwar R, Koterski S, Sweeney G, Sciotti R, Djuric S, Berg C, Trevillyan J, Scherer PE, Rondinone CM, and Klip A.** A dominant-negative p38 MAPK mutant and novel selective inhibitors of p38 MAPK reduce insulin-stimulated glucose uptake in 3T3-L1 adipocytes without affecting GLUT4 translocation. *J Biol Chem* 277: 50386–50395, 2002.
30. **Winder WW and Hardie DG.** AMP-activated protein kinase, a metabolic master switch: possible roles in type 2 diabetes. *Am J Physiol Endocrinol Metab* 277: E1–E10, 1999.
31. **Xi X, Han J, and Zhang JZ.** Stimulation of glucose transport by AMP-activated protein kinase via activation of p38 mitogen-activated protein kinase. *J Biol Chem* 276: 41029–41034, 2001.

Molecular Biology of the Cell
Vol. 16, 3289–3300, July 2005

ELKS, a Protein Structurally Related to the Active Zone-associated Protein CAST, Is Expressed in Pancreatic β Cells and Functions in Insulin Exocytosis: Interaction of ELKS with Exocytotic Machinery Analyzed by Total Internal Reflection Fluorescence Microscopy[V]

Mica Ohara-Imaizumi,* Toshihisa Ohtsuka,†‡ Satsuki Matsushima,§ Yoshihiro Akimoto,‖ Chiyono Nishiwaki,* Yoko Nakamichi,* Toshiteru Kikuta,* Shintaro Nagai,* Hayato Kawakami,‖ Takashi Watanabe,§ and Shinya Nagamatsu*

Departments of *Biochemistry, §Clinical Pathology, and ‖Anatomy, Kyorin University School of Medicine, Mitaka, Tokyo 181-8611, Japan; and †KAN Research Institute, Shimogyo-ku, Kyoto 600-8815, Japan

Submitted September 20, 2004; Revised April 25, 2005; Accepted May 3, 2005
Monitoring Editor: Suzanne Pfeffer

The cytomatrix at the active zone (CAZ) has been implicated in defining the site of Ca^{2+}-dependent exocytosis of neurotransmitters. Here, we demonstrate the expression and function of ELKS, a protein structurally related to the CAZ protein CAST, in insulin exocytosis. The results of confocal and immunoelectron microscopic analysis showed that ELKS is present in pancreatic β cells and is localized close to insulin granules docked on the plasma membrane-facing blood vessels. Total internal reflection fluorescence microscopy imaging in insulin-producing clonal cells revealed that the ELKS clusters are less dense and unevenly distributed than syntaxin 1 clusters, which are enriched in the plasma membrane. Most of the ELKS clusters were on the docking sites of insulin granules that were colocalized with syntaxin 1 clusters. Total internal reflection fluorescence images of single-granule motion showed that the fusion events of insulin granules mostly occurred on the ELKS cluster, where repeated fusion was sometimes observed. When the Bassoon-binding region of ELKS was introduced into the cells, the docking and fusion of insulin granules were markedly reduced. Moreover, attenuation of ELKS expression by small interfering RNA reduced the glucose-evoked insulin release. These data suggest that the CAZ-related protein ELKS functions in insulin exocytosis from pancreatic β cells.

INTRODUCTION

The release of neurotransmitters is restricted to specialized presynaptic membrane compartments called active zones (Landis *et al.*, 1988). The cytomatrix at the active zone (CAZ) is thought to play an organizational role in defining presynaptic sites of synaptic vesicle docking and fusion (Garner *et al.*, 2000). On the other hand, the fusion of vesicles is mediated by the formation of the soluble *N*-ethylmaleimide–sensitive factor attachment protein receptor (SNARE) complex of the presynaptic plasma membrane protein syntaxin 1 and synaptosomal associated protein of 25 kDa (SNAP-25) and the synaptic vesicle protein vesicle-associated membrane protein-2 (Rizo and Südhof, 2002). Although the role of CAZ is understood in neurons, the role of active zones or exocytotic "hot spots" is still unclear in other regulated secretory cells, including pancreatic β cells, where the SNARE complex also plays an important role in their exocytotic processes (Daniel *et al.*, 1999; Nagamatsu *et al.*, 1999).

Recently, several CAZ-related specific proteins in neurons, including Bassoon, RIMs, Munc13s, Piccolo/Aczonin, and CASTs, have been identified and are thought to have a function in synaptic vesicle exocytosis and in the spatial organization of transmitter release (Gundelfinger *et al.*, 2003; Rosenmund *et al.*, 2003). RIM1, a small G protein Rab3A effector, regulates the Ca^{2+}-dependent exocytosis of neurotransmitters in a Rab3A-dependent manner (Wang *et al.*, 1997; Castillo *et al.*, 2002; Schoch *et al.*, 2002). Munc13-1 binds both RIM1 and the target (t)-SNARE syntaxin 1 and is implicated in the priming of synaptic vesicles (Brose *et al.*, 2000; Betz *et al.*, 2001). Bassoon and Piccolo/Aczonin are very large (>400 kDa) and are structurally related CAZ proteins (tom Dieck *et al.*, 1998; Wang *et al.*, 1999). Genetic knockout

This article was published online ahead of print in *MBC in Press* (http://www.molbiolcell.org/cgi/doi/10.1091/mbc.E04–09–0816) on May 11, 2005.

[V] The online version of this article contains supplemental material at *MBC Online* (http://www.molbiolcell.org).

‡ Present address: Department of Clinical and Molecular Pathology, Toyama Medical and Pharmaceutical University, Sugitani, Toyama 930-0152, Japan.

Address correspondence to: Shinya Nagamatsu (shinya@kyorin-u.ac.jp).

Abbreviations used: BSA, bovine serum albumin; CAZ, cytomatrix at the active zone; CCD, charge-coupled device; EPIF, epifluorescence; GFP, green fluorescent protein; KRB, Krebs-Ringer buffer; mAb, monoclonal antibody; pAb, polyclonal antibody; PBS, phosphate-buffered saline; PSF, point spread function; PTD, protein transduction domain; SNAP-25, synaptosomal associated protein of 25 kDa; TIRFM, total internal reflection fluorescence microscopy; t-SNARE, target-soluble *N*-ethylmaleimide–sensitive factor attachment protein receptor.